Dynamics of Fluids near the Critical Point: Decay Rate of Order-Parameter Fluctuations*

Harry L. Swinney†
Physics Department, New York University, 4 Washington Place, New York, New York, 10003

Donald L. Henry
Department of Chemical Engineering, Rice University, Houston, Texas 77001
(Received 25 May 1973)

The decay rate of the order-parameter fluctuations in fluids near the critical point can be determined by measuring the linewidth of the central component in the spectrum of the scattered light, and many such experiments have been reported in the past eight years. In the past two years the dynamical theories developed by Kawasaki and Ferrell to describe the decay rate have been modificed to take into account the anomaly in the shear viscosity and the effect of departures of the correlation function from the Ornstein-Zernike form, and at the same time new accurate measurements of the parameters which enter the theory (the correlation length ξ and the shear viscosity η_s) have been reported. Thus we are able to present here an absolute comparison of the refined mode-mode coupling and decoupled-mode theories with the linewidth data for seven fluids: carbon dioxide, xenon, sulfur hexafluoride, isobutyric acid-water, 3 methylpentane-nitroethane, aniline-cyclohexane, and 2,6 lutidine-water. These linewidth data were obtained in many different laboratories over the past few years; however, in addition to linewidth data previously reported, we also include in our analysis new data which we have obtained for carbon dioxide and xenon and a tabulation and detailed error analysis for all our data for these two fluids. The theories describe only the "critical part" of the decay rate Γ^C; hence the nonanomalous background contributions are first subtracted from the measured linewidths to obtained Γ^C. Then it is shown that the resultant values for a quantity we call the "scaled linewidth," $\Gamma^* \equiv (6\pi\eta_s\Gamma^C/k_BTq^3)$, are described by a single universal curve as a funtion of $q\xi$, for *all* fluids and *every* thermodynamic path that has been investigated near the critical point. This universal curve is described remarkably well by the modified mode-mode-coupling expression of Kawasaki and Lo and the similar decoupled-mode-theory expression of Perl and Ferrell. The accuracy of this comparison, which involves no adjustable parameters, is limited to $\sim 10\%$ by the uncertainties in the background corrections, linewidths, viscosities, and correlation lengths, and by the uncertainties in the various modifications to the theories. The two theories differ significantly only in the extreme nonhydrodynamic region ($q\xi \gg 1$), where the decoupled-mode values for Γ^* are $\sim 10\%$ smaller than those predicted by the mode-mode-coupling theory. Although the available data in the extreme nonhydrodynamic region appear to be described somewhat better by the decoupled-mode theory than the mode-mode-coupling theory, this result is suggestive rather than conclusive since the data in this region are sparse and exhibit considerable scatter.

As a system approaches a critical point the fluctuations of the order parameter become very large as a consequence of the divergence of the generalized susceptibility for the system. For a simple fluid the order parameter is $\rho - \rho_c$ (the difference between the density and the critical density), and the susceptibility is the isothermal compressibility, $\kappa_T \equiv \rho^{-1}(\partial\rho/\partial P)_T = \rho^{-2}(\partial\rho/\partial\mu)_T$ (where μ is the chemical potential and P is the pressure). For a binary mixture the order parameter is $c - c_c$ (the difference between the concentration and the critical concentration), and the susceptibility is given by $(\partial c/\partial\Delta)_{T,P}$, where Δ is the difference between the chemical potentials of the two components, $\Delta = \mu_1 - \mu_2$. The large fluctuations in the order parameter near the critical point cause the intense scattering known as critical opalescence, first observed over 100 years ago.

The spectrum of the light scattered by a fluid near the critical point contains three components, an intense central component known as the Rayleigh line or the quasielastic component, and the Brillouin doublet, two much weaker components (symmetrically shifted with respect to the incident frequency), which arise from scattering from sound waves. In a simple fluid the intense central component arises from the diffusive decay of density fluctuations, while in a mixture this component is caused primarily by the diffusive decay of the concentration fluctuations. In either case, the width of the central component, which is essentially the decay rate of the order-parameter fluctuations, is given (for scattering vector $\vec{q}$) by

$$\Gamma = (L/X)q^2, \tag{1}$$

where L is an Onsager kinetic coefficient and X is a generalized susceptibility. In 1954 Van Hove[1] pointed out that since X diverges strongly as the critical point is approached, while L was pre-

sumed to be constant near the critical point, the decay rate Γ should therefore go to zero as the critical point is approached. This explained the "critical slowing down" that had been frequently reported by experimentalists: as the critical point is approached, systems require increasingly longer times to reach equilibrium.

Direct measurements of Γ were not possible until the mid 1960s when the technique of light-beating or optical-mixing spectroscopy was developed, using a laser as a light source. This technique has been utilized to determine the linewidth Γ of the central component of the scattered light for many fluid systems, and the experiments have revealed much new information about the dynamics of fluids near the critical point. For example, it is now realized that the kinetic coefficient L is not well behaved, as previously presumed, but diverges strongly as the critical point is approached.[2-10] Another result not anticipated when the first linewidth experiments were performed is that very near the critical point, when the range ξ over which the fluctuations in density (or concentration) are correlated becomes so large that $q\xi >> 1$, then Γ depends only on q and is independent of the temperature.

In the late 1960s Kawasaki and Kadanoff and Swift developed the "mode-mode-coupling" theory to describe the dynamics of systems near the critical point; an alternative approach to the calculation of the dynamical properties was taken by Ferrell, whose"decoupled-mode" theory yielded in most cases the same predictions as the mode-mode-coupling theory. Although these theories were rather successful in describing the principal results of the experimental investigations of the dynamics of critical systems, it was nevertheless clear that the theoretical expressions derived for the decay rate were incomplete because the calculations neglected the vertex corrections, the wave number and frequency dependence of the viscosity, and also the effects of departures from Ornstein-Zernike correlations. The extent to which the various corrections would influence the theoretical results was unknown. Moreover, the observed agreement between the Kawasaki-Ferrell expression for the decay rate and the measured linewidths was achieved by adjusting two parameters in the theory.

Recently the major deficiencies in the theories have been rectified by new mode-mode calculations of Lo and Kawasaki and decoupled-mode calculations of Perl and Ferrell. In addition, *absolute* tests of the theories have now become possible because of new independent measurements of the parameters which enter the theories, the correlation length and the shear viscosity. In the present paper we present a comparison of the predictions of the refined mode-mode-coupling and decoupled-mode theories with Rayleigh-linewidth data that have been obtained for seven different fluids in many different laboratories over the past few years; thus the theories are tested for a variety systems, using *no* adjustable parameters.

In Sec. I we review briefly the recent theoretical and experimental developments on the subject of the decay rate of order-parameter fluctuations in fluids near the critical point. In Sec. II we present the results of the new mode-mode calculations of Lo and Kawasaki and the decoupled-mode calculations of Perl and Ferrell. In Sec. III we analyze in detail our CO_2 and xenon linewidth data, with particular attention given to sources of error. In Sec. IV our CO_2 and xenon linewidth data and the linewidth data for five other fluids (obtained in experiments in many laboratories) are compared with the predictions of the refined mode-mode-coupling theory, and in Sec. V the linewidth data are compared with the refined decoupled-mode theory. Finally, in Sec. VI we present the conclusions drawn from our comparison of the results of Rayleigh-linewidth measurements with the theories which have been developed to describe the dynamical behavior of fluids near the critical point.

I. HISTORICAL BACKGROUND

The subject of Rayleigh-linewidth measurements in fluids near the critical point has been reviewed in numerous articles (Benedek,[11] Cummins and Swinney,[12] Chu,[13] Cummins,[14] Swinney, Henry, and Cummins[6]) since the first experiments (Alpert *et al.*,[15] Ford and Benedek[16]) were reported in 1965. Therefore, this section will be mainly limited to a brief discussion of recent developments.

In the hydrodynamic region (where $q\xi << 1$) the spectrum of the light scattered by a fluid can be obtained from a solution of the linearized equations of hydrodynamics.[17] The theory predicts that the central component in the spectrum should have the Lorentzian line shape and a half-width at half-maximum given by

$$\Gamma = \left[\alpha \Big/ \left(\frac{\partial c}{\partial \Delta}\right)_{T,P}\right] q^2 \quad \text{(binary mixture)}, \tag{2a}$$

$$\Gamma = [\lambda/\rho c_p] q^2 \quad \text{(simple fluid)}. \tag{2b}$$

Thus the Onsager coefficients of Eq. (1) are, for a binary mixture and a simple fluid, respectively, the concentration conductivity α and the thermal conductivity λ; the appropriate susceptibility for a simple fluid is the constant-pressure specific

heat c_p, which is proportional to κ_T near the critical point. The magnitude of the scattering vector $\vec{q}$ is given by $q = 2nK_0 \sin\frac{1}{2}\theta$, where n, K_0, and θ are the refractive index, the magnitude of the wave vector of the incident light in vacuum, and the scattering angle, respectively.

Linewidth measurements in simple fluids and mixtures have shown that Γ does approach zero as the critical point is approached, as expected from the Van Hove theory. The asymptotic behavior of the diffusion coefficient $D = \Gamma/q^2$ of a simple fluid at the critical density (or a mixture at the critical concentration) has been found to be described in the hydrodynamic region by a simple exponential law,

$$D \sim \epsilon^{\gamma - \psi}, \tag{3}$$

where $\epsilon \equiv \Delta T/T_c$ (with $\Delta T \equiv |T - T_c|$), and γ and ψ are, respectively, the exponents which characterize the divergences in X and L.

The linewidths measured in five binary mixtures (aniline-cyclohexane,[18,19] isobutyric acid-water,[20] n-hexane-nitrobenzene,[21] phenol-water,[22] and 3 methylpentane-nitroethane[23,24]) were found to be described in the hydrodynamic region by the simple exponential law (3) with $\gamma - \psi \simeq 0.63$, but the exponents that were obtained for the simple fluids CO_2[2] and xenon[4] were somewhat higher, $\gamma - \psi \simeq 0.74$, and for SF_6 the exponent was markedly different, $\gamma - \psi \simeq 1.26$,[11,25] contrary to the expected "universality" in critical behavior.

The larger exponents observed for the pure fluids was a matter of serious concern because the concept of universality was well established from numerous measurements of the static properties of many diverse systems near the critical point. It was suggested that perhaps the linewidth measurements were affected by impurities in the samples, but extensive systematic studies by Bak and Goldburg,[26] (on phenol-water with hypophosphorous acid as an impurity) and by Bak, Goldburg, and Pusey[27] (on bromobenzene-water with acetone as an impurity) showed that even for fairly high impurity concentrations the critical behavior is unchanged, except for a change in T_c.

It was also suggested that the hydrodynamic expression for Γ [Eq. (1)] might not apply near the critical point even when $q\xi \ll 1$; however, there is one fluid, CO_2, for which the diffusivity has been determined in the critical region both by linewidth measurements and by conventional thermodynamic techniques, and in the temperature range common to both sets of data the diffusivities obtained by the different techniques are in excellent agreement, thus corroborating Eq. (1) (see Sec. III C and Ref. 2).

In 1971 Sengers[28] suggested that the apparently higher exponents observed for the pure fluids could be explained by taking into consideration the nondivergent background contribution to the thermal conductivity. Because of the large contribution of nonanomalous background terms, the behavior of systems in the temperature region readily accessible to experiment may be very different from the true asymptotic behavior, which is presumably describable by the simple exponential laws. (See the discussion in the 1967 review by Fisher.[29]) Thus the nonsingular background contributions must first be subtracted if the data are to be analyzed over extended temperature ranges.

Sengers and Keyes[30] found that when the CO_2 data were analyzed with the background thermal conductivity taken into account, the exponent $\gamma - \psi$ was reduced from 0.73 to 0.62, and in a similar analysis of the xenon data we found that $\gamma - \psi$ was reduced from 0.75 to 0.64.[6] However, Benedek *et al.*[31] found that the thermal-conductivity background correction did not bring their SF_6 data into agreement with the results of other fluids (see also Refs. 32 and 33). The SF_6 puzzle has recently been solved by three new independent experiments (Langley and co-workers[34,35]; Lim and Swinney[35]; and Feke, Hawkins, Lastovka, and Benedek[36]), all in agreement with one another and in strong disagreement with the previous SF_6 data. The new SF_6 linewidth data, after subtraction of the background terms, yield $\gamma - \psi = 0.61 \pm 0.04$; hence SF_6 does indeed exhibit the same critical behavior as other fluids.

The occurrence of critical anomalies in the transport coefficients was predicted in 1962 by Fixman from a consideration of the interaction between transport currents and the spontaneous density fluctuations.[37] This concept of Fixman was reconsidered in 1966 by Kawasaki, who proposed a different method of calculation, starting from the correlation-function expressions for the transport coefficients (Kubo formulas).[38] The currents $J(t)$ in the correlation functions for the transport coefficients, $\int \langle J(0)J(t)\rangle\, dt$, were expanded in a power series in the macroscopic variables A_q, whose equations of motion (as well as the coefficients in the power-series expansion) must be deduced from the macroscopic equation of motion. In 1968 Kadanoff and Swift extended Kawasaki's theory and deduced the temperature dependence of the transport coefficients.[39]

In the Kadanoff-Swift-Kawasaki theory the macroscopic normal modes (the "bare propagators") are the solutions to the linearized hydrodynamic equations, and the divergences in the transport coefficients are calculated by considering the breakup on one hydrodynamic mode (a heat flow,

viscous flow, or sound mode) into a multiplicity of other modes, with coupling constants that are obtained by an involved projection-operator technique.[39,40] This approach to the calculation of the critical behavior of the transport coefficients is now called the "mode-mode-coupling theory."

From their mode-mode-coupling calculation, Kadanoff and Swift predicted that D should exhibit the same critical behavior as the inverse correlation length: $D \sim \xi^{-1}$. The divergence of ξ on the critical isochore is described by $\xi = \xi_0 \epsilon^{-\nu}$; hence the prediction was that the exponent $\gamma - \psi$, which describes the critical behavior of the linewidth, should be equal to the exponent ν. The value of $\gamma - \psi$ determined in linewidth measurements agrees well with the value $\nu \simeq 0.63$ obtained from measurements of the angular dependence of the intensity of the scattered light. Thus both theory and experiment indicate that $\gamma - \psi \simeq 0.63$, which, together with the accepted value of γ, $\gamma \simeq 1.23$, yields the exponent characterizing the divergence in the thermal conductivity or concentration conductivity, $\psi \simeq 0.60$. This strong divergence in the conductivity was the first important new result obtained from linewidth measurements near the critical point.

In light-scattering experiments very near the critical point, the range ξ of the fluctuations becomes comparable to q^{-1}, and the ordinary laws of hydrodynamics must be supplanted by a more general dynamical theory. In 1969 Kawasaki[40] used the mode-mode-coupling approach to derive an expression for the linewidth that is applicable over the entire domain from the hydrodynamic region ($q\xi \ll 1$) to the region very near the critical point ($q\xi \gg 1$). The same expression for the linewidth was subsequently derived by Ferrell,[41] whose approach was based on the fluctuation-dissipation theorem. In the Kawasaki-Ferrell equation [Eq. (16), Sec. II] the linewidth is expressed as a function of the shear viscosity η_s and the correlation length ξ.

In 1969 Berge, Calmettes, Laj, and Volochine[18] extended their linewidth measurements on aniline-cyclohexane into the extreme nonhydrodynamic regime, where $q\xi \gg 1$, and subsequently this region has been investigated for other mixtures and simple fluids. The measured linewidths, after the subtraction of the background, have been found to be described well by the Kawasaki-Ferrell expression; however, for most systems this comparison was made taking η_s and ξ (or at least ξ_0) as adjustable parameters, since they were not known from independent measurements (see, e.g., Refs. 4, 18, and 27). On the other hand, in those systems for which independent measurements of ξ and η_s were performed (see, e.g., Refs. 6, 23, and 42) the theory was found to yield linewidth values near T_c larger than those measured if the background viscosity were used for η_s, but the predicted linewidths near T_c would be too small if the theory was interpreted using the full measured macroscopic values of the shear viscosity for η_s.

In the past two years Kawasaki and Lo[43,44] and also Perl and Ferrell[45,46] have considered the problem of the ambiguity in the interpretation of the "high-frequency" shear viscosity that appeared in the decay-rate equation, and they have derived expressions relating the decay rate to the *macroscopic* shear viscosity, thus removing the ambiguity. There have also been two other recent modifications to the theory: (i) Lo and Kawasaki[47] have considered the effect of vertex corrections, which were not included in Kawasaki's original development of the theory, and (ii) Swinney and Saleh[48(a)] have evaluated the Kawasaki-Ferrell decay rate integral for more realistic forms of the correlation function than the Ornstein-Zernike form.

These recent refinements of the theory and new correlation-length and viscosity data obtained within the past year warrant a new analysis of the linewidth data. In the present paper we analyze all the linewidth data for fluids for which independent η_s and ξ data exist, testing particularly the prediction of the mode-mode-coupling theory that a particular dimensionless combination of the measured quantities, $6\pi\eta_s\Gamma^C/k_BTq^3$, where Γ^C is the critical part of the linewidth, should be described by the same universal function of $q\xi$ for all simple fluids and mixtures, for any thermodynamic path.

II. THEORY

A. Background Corrections

The theories recently developed to describe the critical behavior of transport properties near the critical point apply only to the "critical" part of the transport property; therefore, the noncritical "background" contribution to each transport coefficient (which is termed the "bare" kinetic coefficient by Kawasaki) must first be subtracted from the measured properties before the data can be compared with the theoretical predictions. Thus we can write any transport property $L_q(u)$ (where u, for example, could be the temperature or density) as the sum of two terms,

$$L_q(u) = L^B(u) + L_q^C(u), \tag{4}$$

where the background part L^B is the bare kinetic coefficient (the value that L would have in the absence of any critical anomaly), and the critical part L^C is the quantity treated in recent theoretical

developments. In the hydrodynamic region (i.e., for $q=0$ and $\omega=0$) the critical part diverges to infinity or converges to zero as the critical point is approached,

$$L_0^C(u) \to Au^{\phi} \quad (u \to 0^+),$$

where ϕ is the exponent that characterizes the singularity and A is the amplitude of the singularity. As the region very near the critical point (where $q\xi \gtrsim 1$) is approached, L^C will in general become q dependent; this is indicated explicitly by the q subscripts in Eq. (4).

The partition of a transport coefficient into background and critical parts is clearly a crucial part of the data analysis in any experimental investigation of the dynamics of a system near the critical point. In such experiments (which include, for example, measurements of the spin-diffusion rate in magnets and the sound velocity and attenuation in fluids, as well as measurements of the viscosity, conductivity, and diffusivity), a meaningful comparison between theory and experiment can be made only if a systematic procedure can be developed for estimating the bare Onsager kinetic coefficient. For the thermal conductivity and shear viscosity of a pure fluid, Sengers and Keyes[30] have developed a method for estimating λ^B and η_s^B using data obtained far from the critical point. The procedure is based on the empirical result, frequently used in the engineering literature, that the "excess" thermal conductivity,

$$\tilde{\lambda}(\rho) = \lambda(\rho, T) - \lambda(0, T) \tag{5}$$

[where $\lambda(\rho, T)$ is the thermal conductivity at a density ρ and temperature T and $\lambda(0, T)$ is the thermal conductivity in the dilute gas limit], is independent of temperature for temperatures and densities up to approximately twice the critical temperature and density. The Sengers-Keyes ansatz is that the background thermal conductivity in the critical region is given by

$$\lambda^B(\rho, T) = \tilde{\lambda}(\rho) + \lambda(0, T), \tag{6}$$

where $\tilde{\lambda}(\rho)$ is determined using data obtained *away* from the critical region. A similar expression is assumed to hold for the background viscosity.

Linewidth measurements indicate that the background contribution to the conductivity is far less important for mixtures than for pure fluids, and de Gennes[48(b)] has argued that this is plausible on physical grounds. It seems reasonable to expect that expressions analagous to Eqs. (4) and (5) should apply to the concentration conductivity $\alpha(c,T)$ as well as to the thermal conductivity; however, there are no measurements of $\alpha(c,T)$ from which $\tilde{\alpha}(c,T)$ and $\alpha^B(c,T)$ can be computed. In the absence of any means of estimating $\alpha^B(c, T)$, the linewidths measured for mixtures have, with one exception, all been analyzed, assuming, as we will assume in our analysis of the linewidth data for mixtures, that $\alpha^B(c, T)=0$. The only authors who have considered the effect of a nonzero bare Onsager kinetic coefficient on linewidth data for mixtures were Chang *et al.*,[23] who found that if α^B were taken as a free parameter, then the fit of their linewidth data for 3 methylpentane-nitroethane to the mode-mode-coupling theory would be significantly better with nonzero α^B than with $\alpha^B=0$; however, this conclusion should be revised because the mode-mode-coupling theory has been refined subsequent to this analysis.

Now let us consider the form of the decay-rate equation with the background contributions taken into account, separating L into background and critical parts:

$$\Gamma = (L^B/X_q)q^2 + (L_q^C/X_q)q^2. \tag{7}$$

The susceptibility can also be written as the sum of background and critical parts,[49]

$$X_q = X^B + X_q^C.$$

We will assume that the q dependence of X_q^C is given by the Ornstein-Zernike form,

$$X^C(q) = X^C(q=0)/(1+q^2\xi^2), \tag{8}$$

and we further assume, as is indicated by the susceptibility and correlation-length data for simple fluids and mixtures, that $X^B \ll X_q^C$ when $q\xi \gtrsim 1$. Then Eq. (7) becomes

$$\Gamma = (L^B/X)q^2(1+q^2\xi^2) + \Gamma^C(X^C/X), \tag{9}$$

where

$$\Gamma^C \equiv (L_q^C/X_q^C)q^2, \tag{10}$$

and the absence of q subscript on X in (9) indicates the $q=0$ or thermodynamic quantity.

Equation (9) is our working equation. The measured linewidth values Γ together with independent data for X, L^B, and ξ will be substituted into (9) to deduce values for Γ^C, which will then be compared with the theoretical predictions. The partition of X into critical and background parts is somewhat arbitrary; however, over the temperature range of the linewidth data X and X^C are equal within a few percent (see Sec. III D), so this is a small correction, unlike the separation of the thermal conductivity into critical and background parts. In discussing the full linewidth Γ we shall at times refer to the first term on the right-hand side of (9) as the "background part" of the linewidth and the second term as the "critical part," even though the "critical part" should

properly refer only to Γ^C [Eq. (10)].

For future reference we now write (9) separately in the notation for simple fluids,

$$\Gamma = (\lambda^B/\rho c_p) q^2 (1 + q^2 \xi^2) + \Gamma^C (c_p^C/c_p), \tag{11a}$$

and for binary mixtures,

$$\Gamma = \left(\frac{\alpha^B}{(\partial c/\partial \Delta)_{T,P}}\right) q^2 (1 + q^2 \xi^2) + \Gamma^C \left[\left(\frac{\partial c}{\partial \Delta}\right)^C_{T,P} \Big/ \left(\frac{\partial c}{\partial \Delta}\right)_{T,P}\right]. \tag{11b}$$

[As before, the meaning of the 3 C's is (i) c_p, specific heat; (ii) superscript C, "critical"; (iii) c in $(\partial c/\partial \Delta)$, concentration.]

B. Dynamic Scaling

The static-scaling-law ideas of Widom[49] and Kadanoff[50] were extended into the domain of dynamics in 1967 by Ferrell *et al.*,[51] who treated the problem of the λ transition in superfluid helium. Subsequently, Halperin and Hohenberg[52] generalized the dynamic-scaling approach and applied it to the gas-liquid critical point and other critical systems. Recently, Hankey and Stanley[53] have shown that both static and dynamic scaling follow from a generalized homogeneous function hypothesis.

Halperin and Hohenberg assume that the characteristic frequency of a system near the critical point is described by a homogeneous function of q and ξ^{-1}. Near the critical point of a fluid the dominant collective mode is the diffusive decay of the order-parameter fluctuations; in this limit the decay rate Γ is the characteristic frequency that is given in the dynamic scaling theory by

$$\Gamma = f(q, \xi^{-1}) \equiv q^z f(1, 1/q\xi), \tag{12}$$

where z is the degree of homogeneity of f. The known form of Γ in the hydrodynamic region, $\Gamma = (L/X) q^2$, leads to $z = 2 + (\gamma - \psi)/\nu$ where, as before, γ, ψ, and ν characterize the divergences in X, L, and ξ, respectively, as the critical point is approached along either side of the coexistence curve or along the curve corresponding to the critical density of concentration. (In general, the exponents could be different for the three paths, but they are the same if static scaling is assumed.)

In the most general treatment of dynamic scaling the behavior of the function f is completely unspecified beyond the statement in Eq. (12). However, it is frequently assumed that $f(q, \xi^{-1})$ is well behaved for all (q, ξ^{-1}), except at the origin, an assumption which yields for $q\xi \gg 1$

$$\Gamma = B q^z, \tag{13}$$

where the constant B applies both above and below T_c, everywhere within the region $q\xi \gg 1$.

C. Mode-Mode-Coupling Theory

The integral expression for the decay rate derived by Kawasaki[40] from a consideration of the coupling between the different hydrodynamic modes near the critical point is

$$\Gamma^C = \frac{k_B T}{(2\pi)^3 \eta_s^*} \int d\vec{k} \left[\left(\frac{q}{k}\right)^2 - \left(\frac{\vec{q}\cdot\vec{k}}{k^2}\right)^2\right] \frac{\hat{G}(\vec{q} - \vec{k})}{\hat{G}(\vec{q})}, \tag{14}$$

where $\hat{G}(\vec{q}) = \int d\vec{k} G(\vec{r}) e^{i\vec{q}\cdot\vec{r}}$, and $G(\vec{r})$ is the density-density (or concentration-concentration) correlation function; η_s^* is the "high-frequency" shear viscosity, and k_B is Boltzmann's constant. Kawasaki evaluated the integral in (14) using the Ornstein-Zernike (OZ) form for the correlation function,

$$\hat{G}_{OZ}(\vec{q}) \propto (\xi^{-2} + q^2)^{-1}, \tag{15}$$

obtaining

$$\Gamma^C = (k_B T/6\pi\eta_s^* \xi^3) K_0(q\xi), \tag{16a}$$

where

$$K_0(x) = \tfrac{3}{4}[1 + x^2 + (x^3 - x^{-1}) \arctan x]. \tag{16b}$$

[In (15) and in subsequent expressions for the correlation function, we omit proportionality factors independent of $\vec{q}$ or $\vec{r}$, since they cancel in (14).]

As mentioned previously, there is an ambiguity in the interpretation of η_s^* in Eqs. (14) and (16). In the integral expression that Kawasaki originally derived for the decay rate, the viscosity appears in the integrand; the simplified expression [Eq. (14)] was obtained by replacing the wave-vector and frequency-dependent viscosity by the constant η_s^*, which is an effective weighted average over all viscous modes appearing in the intermediate states.[40] The correct interpretation of η_s^* requires a self-consistent evaluation of both the viscosity and the decay rate. Kawasaki and Lo first solved the simultaneous integral equations involving the viscosity and decay rate with the frequency dependence of the viscosity neglected, but the nonlocality included.[43] Recently Lo and Kawasaki have extended this calculation, investigating the importance of the frequency dependence or memory effects, and they have deduced an expression which relates η_s^* to the macroscopic shear viscosity η_s, thus removing the ambiguity in the shear viscosity.[44] They find

$$\eta^{*-1} = R(q\xi) \eta_s^{-1}, \tag{17a}$$

where

$$R(x)=[K(x)+\Delta K(x)]/K_0(x). \quad (17b)$$

The term $K(q\xi)/K_0(q\xi)$, which describes the effect of nonlocality on the viscosity ($K/K_0=1$ if nonlocal effects are neglected), is given numerically in Fig. 3 of Kawasaki and Lo,[43] and $\Delta K(q\xi)/K_0(q\xi)$, which describes the effect of the frequency dependence is given in Table I of Lo and Kawasaki.[44] The viscosity correction factor $R(q\xi)$ is shown in Fig. 1, curve (a). Note that η_s^* differs from η_s even far from T_c; in that region $\eta_s^*=\eta_s/1.063$.

In Kawasaki's analysis of the order-parameter fluctuations in a fluid, Dyson-type self-consistent equations for the time correlations of the critical fluctuations were derived, and Eq. (14) was then obtained by evaluating the contributions of the two lowest-order terms to the decay rate. Recently Lo and Kawasaki[47] have investigated the contributions of the four next-higher-order terms and have found that the inclusion of these "vertex-correction" terms reduces Eq. (14) by 2.44% for $q\xi\ll1$ and increases (14) by 0.40% for $q\xi\gg1$. The vertex correction $V(q\xi)$, the ratio of the corrected to the uncorrected decay rate, is shown by curve (b) in Fig. 1, which was obtained by connecting the limiting values of $V(q\xi)$, $V(\infty)$ and $V(0)$, by a smooth curve. [A calculation of this small modification to the theory for intermediate values of $q\xi$ would require the evaluation of a complicated integral expression—Eq. (2.10) in Ref. 47]. The vertex correction to the decay rate is frequency dependent, with the above values for $q\xi\ll1$ and $q\xi\gg1$ applying only in the zero-frequency limit. Because of the frequency dependence of the vertex correction, the observed spectral line will in principle deviate from the Lorentzian line shape, but the correction is so small that the predicted departures from the Lorentzian shape would be very difficult to observe.

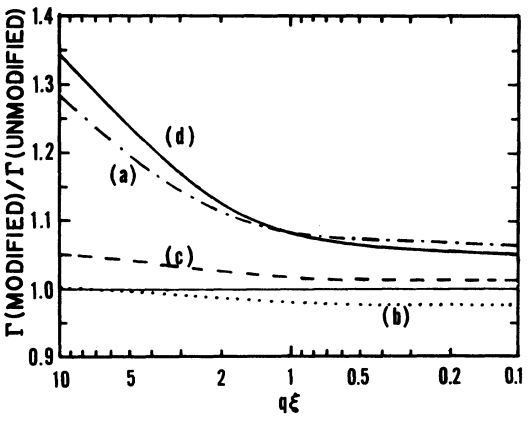

FIG. 1. The ratio of the modified to the unmodified theoretical decay rate is shown for three modifications to the mode-mode-coupling theory: (a) $R(q\xi)$, the viscosity correction [Kawasaki and Lo (Ref. 44)]; (b) $V(q\xi)$, the vertex correction [Lo and Kawasaki (Ref. 46)]; (c) $C(q\xi)$, the effect of departures of the correlation function from the Ornstein-Zernike form, calculated for the Fisher-Burford correlation function with $\eta=0.1$ [Swinney and Saleh (Ref. 48)]; (d) $H(q\xi)=R(q\xi)V(q\xi)C(q\xi)$, the combined effect of the viscosity, vertex, and correlation-function modifications.

D. Decoupled-Mode Theory

Ferrell has calculated the critical behavior of transport properties by factoring the currents $J(t)$ in the current correlation functions in the Kubo formulas, and then the Kubo formulas were evaluated directly, a procedure which, as Ferrell has pointed out, is equivalent to the mode-mode-coupling theory without vertex corrections because the absence of internal lines (the vertex corrections) between two intermediate-state propagators allows them to be factored within the Kubo integral.[41] Ferrell obtained for the critical part of the decay rate

$$\Gamma^C=\frac{k_BTq^2}{8\pi\eta_s^*\hat{G}(\vec{q})}\int d\vec{r}\left(\frac{1}{r}+\frac{(\vec{q}\cdot\vec{r})^2}{q^2r^3}\right)G(\vec{r})e^{i\vec{q}\cdot\vec{r}}, \quad (18)$$

where η_s^* is a constant, wave-number-independent viscosity.[41] If the Ornstein-Zernike form is used for the correlation function,

$$G_{OZ}(\vec{r})\propto[\exp(-r/\xi)]/r, \quad (19)$$

then Eq. (18) yields the same result [Eq. (16)] that Kawasaki obtained with the mode-mode-coupling theory.[41,48(a)]

The fluctuation-dissipation or Kubo formulas for the viscosity and decay rate are a pair of coupled equations that in principle can be solved self-consistently to obtain $\eta_s(q,\omega)$ and $\Gamma^C(q)$. However, since the viscosity is only weakly dependent on q, ω, and ϵ, a good first approximation for Γ^C can be obtained by replacing $\eta_s(q,\omega)$ in the decay-rate integral by a constant, "η_s^*"; this was the procedure followed in obtaining Eq. (18).[41] A more accurate expression for Γ^C can of course be obtained by solving iteratively the coupled equations for η_s and Γ^C. Recently, Perl and Ferrell[45,46] have considered an alternative to such a direct attack on the coupled equations, and they have shown that their approach leads to a self-consistent refined expression for Γ^C. Perl and Ferrell began with the observation that the linewidth data for 3 methylpentane-nitroethane are fairly accurately described by the empirical expression

$$\Gamma^C = (k_B T/16\bar{\eta}_s) q^2 (q^2 + \xi^{-2})^{1/2}, \tag{20a}$$

where $\bar{\eta}_s$ is an adjustable parameter.[45,46] This expression for Γ^C was then used in evaluating the Kubo integral for $\eta_s(q, \omega)$, which in the hydrodynamic limit was found to have a critical part given by

$$\eta_s^C \equiv \eta_s^C(q=0, \omega=0) = (8\bar{\eta}_s/15\pi^2) \ln(q_D \xi), \tag{20b}$$

where q_D is a free parameter to be determined by fitting the macroscopic shear-viscosity data to Eq. (20b). [Equation (20b) was also derived by Kawasaki.[43]] Finally, Perl and Ferrell used their result for $\eta_s(q, \omega)$ to evaluate the decay-rate integral, obtaining the following refined expression for Γ^C:

$$\Gamma^C = (k_B T/6\pi \eta_s^{\text{eff}} \xi^3) K_0(q\xi), \tag{21a}$$

where

$$\eta_s^{\text{eff}} = \eta_s^B \left\{ 1 + \frac{\bar{\eta}_s}{\eta_s^B} \left(\frac{8}{15\pi^2} \right) \left[\ln \left(\frac{q_D \xi}{(1+q^2\xi^2)^{1/2}} \right) + \tau(q\xi) \right] \right\} \tag{21b}$$

and $\tau(q\xi)$ is a function given numerically.[46] [Some values of the function τ, which increases montonically with increasing $q\xi$, are $\tau(0) \simeq \tau(0.1) = -0.492$, $\tau(1) = -0.357$, $\tau(2) = -0.189$, and $\tau(\infty) \simeq \tau(100) = 0.090$.]

Equation (21a) can be rewritten as

$$\Gamma^C = \frac{k_B T}{6\pi \eta_s^B} [q^2 (q^2 + \xi^{-2})^{1/2}] \frac{\sigma(q\xi)}{\theta(q\xi)}, \tag{21c}$$

where

$$\sigma(x) = \tfrac{3}{4}(1+x^2)^{1/2} \left[\frac{1}{x^2} + \left(\frac{1}{x} - \frac{1}{x^2} \right) \arctan x \right]$$

is Ferrell's "dynamical scaling function,"[41] which increases monotonically with increasing $q\xi$, varying from $\sigma(0) = 1$ to $\sigma(\infty) = \frac{3}{8}\pi = 1.178$, and $\theta(q\xi)$ is the function which describes the q dependence of η_s^{eff},

$$\theta(x) = 1 + \frac{\bar{\eta}_s}{\eta_s^B} \left(\frac{8}{15\pi^2} \right) \left[\ln \left(\frac{x q_D/q}{(1+x^2)^{1/2}} \right) + \tau(x) \right].$$

The result of the Perl-Ferrell calculation is that the effective viscosity has a weak q dependence, similar to that of $\sigma(q\xi)$, i.e., $\sigma(q\xi)/\theta(q\xi) \simeq$ const. Thus the refined theory [Eq. (21c)] predicts that the empirical expression, Eq. (20a), should describe the linewidth data within a few percent, so the calculation is self-consistent.

In Sec. V linewidth and viscosity data are used to deduce $\bar{\eta}_s$ and q_D, respectively, and then the refined decoupled-mode expression [Eq. (21)] is compared with the results of linewidth measurements for different fluids.

E. Correlation-Function Modification

The integral expressions (14) and (18) for the decay rate were evaluated using the Ornstein-Zernike form for the correlation function, but scattering experiments and the theoretical investigations of the Ising model by Fisher and Burford[54] have shown that there are small departures from Ornstein-Zernike behavior near the critical point. The correct asymptotic form for the correlation function at the critical point is expected to be $r^{-(1+\eta)}$, with $\eta \simeq 0.05$ to 0.1, while for the Ornstein-Zernike theory $\eta = 0$.

Fisher and Burford[54] (FB) found that correlations in the Ising model are accurately described by

$$\hat{G}_{\text{FB}} \propto (\xi^{-2} + \phi^2 q^2)^{\eta/2} / [\xi^{-2} + (1 + \tfrac{1}{2}\eta\phi^2) q^2], \tag{22}$$

where $\phi = 0.15 \pm 0.01$, independent of the type of lattice. Swinney and Saleh[48] have evaluated the decay-rate integral using $\hat{G}_{\text{FB}}$, and the result for the decay-rate ratio,

$$C(q\xi) = \Gamma^C(\hat{G}_{\text{FB}}, q\xi)/\Gamma^C(\hat{G}_{\text{OZ}}, q\xi), \tag{23}$$

is given by curve (c) in Fig. 1 for $\eta = 0.1$. The decay-rate integral was also evaluated by Swinney and Saleh[48] and by Chang *et al.*[24] for other forms of the correlation function which have been used in the analysis of data from scattering experiments; however, $\hat{G}_{\text{FB}}$ is more satisfactory theoretically since, as explained in Ref. 54, it leads to the correct asymptotic behavior at large r both at the critical point and away from the critical point.

F. Mode-Mode-Coupling Theory with Modifications

With the viscosity, vertex, and correlation-function modifications included, the expression for the decay rate (16) in the mode-mode-coupling theory becomes

$$\Gamma^C = (k_B T/6\pi\eta_s \xi^3) K_0(q\xi) H(q\xi), \tag{24}$$

where the correction factor $H(q\xi)$, which most analyses of linewidth data have heretofore assumed to be unity, is given by

$$H(q\xi) \equiv R(q\xi) V(q\xi) C(q\xi), \tag{25}$$

and is plotted as curve (d) in Fig. 1. Although the vertex correction has not been evaluated for intermediate values of $q\xi$, and the correlation-function correction is somewhat uncertain because the correct form for the correlation function is not well established, these two corrections are nevertheless both small, and we will consider them as well as the nonlocal shear-viscosity correction in our data analysis.

In the hydrodynamic limit $q\xi \ll 1$, the function K_0 simplifies to $K_0(x) = x^2$ and (24) becomes

$$\Gamma^C = 1.052(k_B T/6\pi\eta_s \xi)q^2, \tag{26}$$

which, if the temperature dependence of η_s is neglected, is in accord with the Kadanoff and Swift[39] prediction $\Gamma^C/q^2 \sim \xi^{-1}$.

In the opposite limit, $q\xi \gg 1$, $K_0(x) = (\frac{3}{8}\pi)x^3$, and (24) becomes

$$\Gamma^C = \left(\frac{k_B T}{16\eta_s}\right) R(q\xi) q^3. \tag{27}$$

Although Kawasaki and Lo find that $R(q\xi)$ is increasing fairly rapidly even for $q\xi = 20$ [where $R(q\xi)$ is equal to 1.38], $R(q\xi)$ is expected[55] to approach a constant in the extreme $q\xi \gg 1$ limit. In the intermediate region where $q\xi \leq 1$, K_0 becomes $K_0(x) = x^2(1 + \frac{3}{5}x^2)$; whence

$$\Gamma^C = (k_B T/6\pi\eta_s) q^2(1 + \tfrac{3}{5} q^2\xi^2) H(q\xi). \tag{28}$$

This equation has sometimes been used[56,57] in the past to determine ξ from the slope of plots of Γ^C/q^2 vs q^2, with $H(q\xi)$ implicitly assumed to be constant; however, it is now clear that this procedure is not valid, since $H(q\xi)$ is rapidly varying in this region (see Fig. 1).

In the mode-mode-coupling theory the macroscopic shear viscosity η_s can exhibit an *apparent* logarithmic divergence over some range of temperatures, but η_s is expected to remain finite at the critical point. It is difficult to distinguish experimentally between a weak divergence and a cusp at the critical point; existing viscosity data can be fit equally well to either a cusp or a weak divergence.[58-63] If the viscosity does remain finite at the critical point, then (24) satisfies the dynamic scaling assumption (12) with the degree of homogeneity given by $z = 3$.

A cusped behavior for the viscosity is described by

$$\eta_s = A_0 + A_1 \xi^{-a} + \ldots, \tag{29}$$

where $a > 0$. The dynamic scaling expression (12) presumably describes the decay rate in the limit in which higher-order terms such as the A_1 term in (29) are negligible. Since the A_1 term in (29) is clearly important in the temperature range of existing linewidth data, it is difficult to test a general functional form such as the dynamic scaling expression (12). On the other hand, since independent viscosity and correlation-length data have been obtained for several fluids near the critical point, the mode-mode-coupling expression (24) can be tested directly with no adjustable parameters. (This is a valid test of the theory only if the assumed form for the background subtractions is correct.)

The equation for the critical part of the linewidth (24) can be rewritten as

$$\Gamma^* = (1/q\xi)^3 K_0(q\xi) H(q\xi), \tag{30a}$$

where the "scaled" linewidth Γ^* is defined as

$$\Gamma^* \equiv (6\pi\eta_s/k_B T)(\Gamma^C/q^3). \tag{30b}$$

Thus the theory predicts that the experimental data for Γ^* [Eq. (30b)] for different temperatures and scattering angles, obtained for various simple fluids and binary mixtures, should all fall on a *single universal* curve [Eq. (30a)] when the (dimensionless) quantity Γ^* is plotted as a function of $q\xi$. This single curve is predicted to describe the critical behavior not only along the critical isochore and the coexistence curve, but also along *any* other thermodynamic path in the critical region. In Sec. IV we test the mode-mode-coupling prediction for all fluids for which ξ and η_s have been independently determined.

III. XENON AND CO_2 EXPERIMENTS

In this section we discuss the Rayleigh-linewidth experiments performed in our laboratory on xenon and carbon dioxide along the critical isochore and along the coexistence curve. The experimental details discussed in Sec. III A apply to both fluids, except as noted. The experimental results are reported in Sec. III B, and are compared with other diffusivity and linewidth measurements on xenon and CO_2 in Sec. III C. Sources of auxiliary data which are used in the linewidth-data analysis (Secs. IV and V) are discussed in Sec. III D.

A. Experimental Details

The lot analyses provided by the suppliers of the fluids indicated an impurity content of less than 30 ppm for the xenon samples and less than 50 ppm for the CO_2 samples.

Each sample cell, formed from 6×6-mm square-bore heavy-wall Pyrex tubing with a capillary attached to one end, was evacuated and then filled cryogenically with fluid. The capillary was permanently sealed with a gas torch. Two samples of fluid were used in the xenon experiment: the first was used for most of the data above T_c[4,5,6] and the second for the data along the coexistence curve,[8,10] although some measurements were also performed above T_c with the second sample. In the CO_2 experiments two samples were also used. All of the CO_2 data obtained with the second sample and much of the data obtained for the second xenon sample have not been previously reported. For each fluid there was no detectable dependence of the results on the sample used.

The mean density of fluid in the cell relative to the critical density was determined by observing the change in height of the meniscus with temperature over a 20-K range and comparing the results to the height dependence as a function of relative mean density calculated from independent density data.

Using the density data of Garside *et al.*[64] (see also Cornfield and Carr[65]), we found from measurements of the meniscus height that the density of the first xenon sample was $0.3 \pm 0.1\%$ below the critical density, and the density of the second sample was $3.2 \pm 0.3\%$ above the critical density. The mean density of the primary CO_2 sample was $0.3 \pm 0.1\%$ above the critical density, as determined using the Guggenheim[66] corresponding-states relation. The density of the second CO_2 sample was not measured, but this sample was used only very near $T_c (T > T_c)$, where the location of the critical isochore was determined from linewidth measurements as a function of height.

The sample cell was suspended in a temperature-controlled oil bath having an index of refraction matched to the glass cell to 1 part in 10^4 at 6328 Å near the critical temperature of the fluid. The temperature of the oil bath was maintained to ± 0.0005 K for periods of days for measurements on the second xenon sample.

Gravitationally induced density gradients near the critical temperature made it necessary to measure the linewidth as a function of height in the sample cell, and the minimum in the linewidth as a function of height (at a fixed temperature and scattering angle) was taken to be the value on the critical isochore.[2] Curve (a) in Fig. 2 shows the height dependence of the linewidth for xenon at a scattering angle of 90° for $\Delta T = 0.018$ K; the averaging due to the finite beam diam (0.2 mm) is small at this temperature but becomes significant at temperatures within a few millidegrees from T_c. No height dependence of the linewidth was observable far from T_c, as curve (b) in Fig. 2 illustrates, but height scans were necessary in all measurements within 0.2 K from T_c.

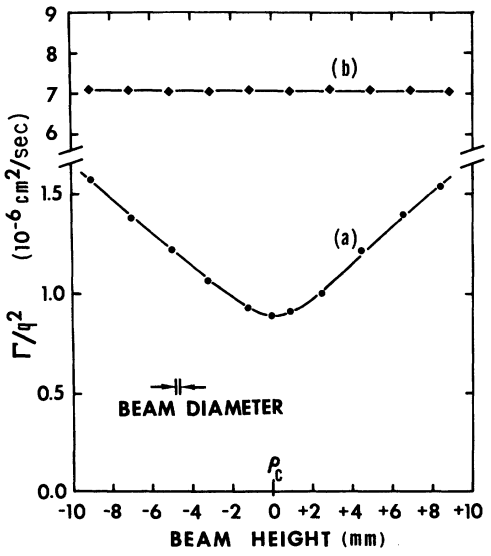

FIG. 2. Γ/q^2 as a function of the beam height in the xenon sample cell ($\theta = 90°$). The linewidth minimum is assumed to correspond to the critical isochore. (a) $\Delta T = 0.018$ K; (b) $\Delta T = 0.700$ K.

The uncertainties in the mean densities of our samples had negligible effect on measurements in the hydrodynamic region, where the linewidth is only weakly dependent on density (cf. Fig. 8 of Ref. 67). Furthermore, in the critical region a minimum in the linewidth as a function of height could always be located so that the mean density was unimportant. Hence the uncertainties in the mean densities had little effect on the linewidth measurements.

Temperature differences were measured with a Fenwal ceramic thermistor whose resistance was measured to 2 parts in 10^5 with a Wheatstone bridge; the thermistor was calibrated against a mercury thermometer having 0.01-K divisions. The precision of the temperature measurements was ± 0.0005 K and the absolute accuracy was ± 0.02 K. The critical temperature was periodically checked by observing the formation of a meniscus as the temperature was very slowly (over periods of several days) lowered to the critical point, and this value was reproducible to ± 0.0005 K. The critical temperature of the first xenon sample, as determined by the mercury thermometer, was 289.756 ± 0.020 K; for the second xenon sample, $T_c = 289.760 \pm 0.020$ K. For both of the carbon dioxide samples T_c was measured to be 304.23 ± 0.02 K. We want to emphasize that although there is an uncertainty of ± 0.02 K in the absolute value of T_c for our samples, the important quantity ΔT was measured with an accuracy of ± 0.0005 K.

The primary source of uncertainty in the scattering angle was the goniometer; alignment of the goniometer with the forward-scattered laser beam (at $\theta = 0°$) was hindered by the spreading of the transmitted beam by the oil bath, which acted as a cylindrical lens. The uncertainty in q ranged from 0.9% at the smallest angle used in the experiments to 0.2% at the largest angle.

We used the data of Smith and co-workers[64,68] for the refractive index of xenon along the critical isochore and along the coexistence curve; they found $n_c = 1.1366$ at 6328 Å. For CO_2, Levelt Sengers, Straub, and Vicentini-Missoni[69] reported

measurements of the refractive index at 5893 Å as a function of density near the critical point; those data, corrected for dispersion using the data of Michels and Hamers,[70] yield $n_c = 1.1074$ at 6328 Å.

The linewidths were measured using the light-beating technique.[11,12,16] Light from a He-Ne laser was focused onto the sample cell, and the light scattered at an angle θ was collected through a slit immediately in front of a lens that focused the light onto a pinhole aperture in front of a photomultiplier. The amplified photocurrent was processed with a spectrum analyzer, whose output was recorded on a strip chart recorder. For a description of the data-reduction techniques used in these experiments, see Refs. 3 and 5.

Some of the xenon measurements above T_c were made with a 60-channel digital-pulse autocorrelator,[71] which gave results in agreement with the spectrum-analyzer measurements within the experimental uncertainty.[10] With favorable signal conditions the linewidths measured with our spectrum-analyzer system are reproducible to within ±3%, while linewidths determined with the correlator are repeatable within ±1% or better.

At the beginning of the xenon work it was discovered that a significant amount of light scattered elastically from the inside walls of the sample cells was acting as a "local-oscillator" signal, mixing with the light scattered from the fluid and producing a "beat" spectrum with a linewidth less than the true "self-beat" linewidth. Figure 3 shows the linewidth as a function of horizontal distance along the scattering volume at a 30.4° scattering angle for $\Delta T = 1.5$ K. The scattering volume was 6 mm long and the optical-collection apertures selected a portion 0.2 mm long. Near the center of the cell the scattering from the cell walls is negligible and Γ/q^2 has the same value as measured at $\theta = 90°$, as the horizontal dashed line indicates. (The cell-wall scattering problem is minimized for $\theta = 90°$, but measurements at this angle were limited by signal-to-noise problems to the region $\Delta T \lesssim 2$ K.) For scattering volumes near the cell walls the intensity of the local oscillator signal was much greater than the sample scattering intensity, and hence the linewidth should become equal there to one-half the self-beat value[12]; the data in Fig. 3 exhibit this behavior. Although there is a plateau region in the center portion of this graph where cell-wall scattering is negligible, the width of the plateau decreases as ΔT is increased, and this imposes an upper bound on the range of ΔT that can be studied by the self-beat technique using our sample cells. For the xenon measurements made with the second sample above $\Delta T = 1$ K, horizontal scans were made at each temperature, and data were selected only from the region of the plateau.

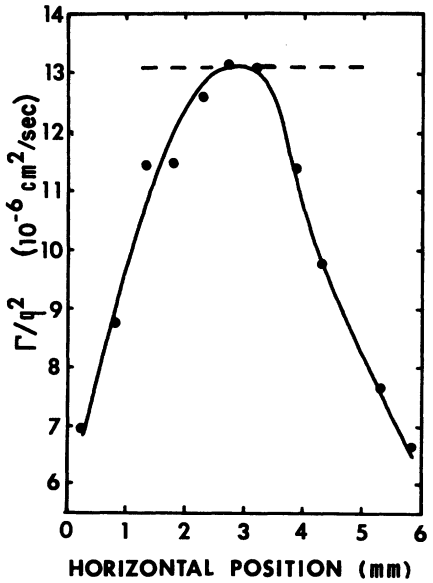

FIG. 3. Γ/q^2 as a function of the horizontal position of the xenon sample cell for $\theta = 30.4°$ and $\Delta T = 1.5$ K. The linewidth decreases sharply for scattering volumes near the cell walls (at the horizontal positions 0 and 6 mm) as a consequence of the intense scattering from the walls. The horizontal dashed line shows the value of Γ/q^2 measured at the same temperature for $\theta = 90°$.

Although in principle one can detect the presence of cell-wall scattering by testing the goodness of the fit of the spectra to a single Lorentzian (or the correlation function to a single exponential), we find from measurements such as those illustrated in Fig. 3, and also from tests with computer-synthesized data, that the wall scattering can be intense enough to produce an error of several percent or more in the linewidths and yet a spectrum will still fit a single Lorentzian within the experimental uncertainty.[72] In general, all linewidth measurements should be carefully examined to determine whether or not scattering from the cell walls or from large dust particles in the sample has resulted in measured linewidths which are smaller than the true linewidths.

B. Experimental Results

Our linewidth data for xenon and CO_2 are listed in Tables I and II, respectively, and Γ/q^2 is plotted as a function of ΔT in Fig. 4 (xenon) and Fig. 5 (CO_2). Table I and Fig. 4 include the xenon data for $T < T_c$ obtained by Lim and Swinney.[8,10] Also shown in Figs. 4 and 5 are a few representative data points obtained in other experiments;

TABLE I. Rayleigh linewidth Γ for xenon as a function of the temperature difference ΔT and the magnitude of the scattering vector q.

Γ (10^5 rad/sec)	ΔT (K)	q (10^5 cm^2/sec)	Γ (10^5 rad/sec)	ΔT (K)	q (10^5 cm^2/sec)
A. Critical isochore					
2.474	5.836	0.809	0.246	0.276	0.809
2.387	5.569	0.809	0.903	0.256	1.596
2.351	5.569	0.809	0.817	0.217	1.596
2.211	5.051	0.809	0.208	0.217	0.809
2.220	5.051	0.809	0.658	0.159	1.596
1.911	4.541	0.809	0.654	0.159	1.596
1.943	4.541	0.809	0.162	0.159	0.809
8.884[a]	4.430	1.596	0.159	0.159	0.809
1.855	4.277	0.809	0.172	0.147	0.809
1.851	4.277	0.809	0.941	0.147	1.917
7.523[a]	3.345	1.596	1.149	0.147	2.107
1.588	3.305	0.809	1.136	0.147	2.107
1.552	3.305	0.809	0.165	0.147	0.809
5.888[a]	2.810	1.596	0.622	0.134	1.596
1.327	2.780	0.809	0.602	0.134	1.596
5.844[a]	2.750	1.596	0.148	0.134	0.809
1.317	2.474	0.809	0.147	0.127	0.809
4.873[a]	2.265	1.596	0.145	0.127	0.809
1.121	2.134	0.809	1.032	0.127	2.107
1.127	2.134	0.809	1.021	0.127	2.107
4.427[a]	2.075	1.596	0.974	0.126	2.107
1.108	1.982	0.809	0.567	0.124	1.596
4.350[a]	1.960	1.596	0.549	0.124	1.596
4.028[a]	1.645	1.596	0.311	0.124	1.191
3.540	1.568	1.596	0.144	0.124	0.809
0.876	1.568	0.809	0.147	0.124	0.809
0.816	1.366	0.809	1.002	0.124	2.107
3.268[a]	1.360	1.596	1.022	0.124	2.107
3.116	1.280	1.596	0.838	0.124	1.917
0.753	1.280	0.809	0.533	0.102	1.596
2.843[a]	1.215	1.596	0.282	0.102	1.191
3.108[a]	1.210	1.596	0.122	0.102	0.809
2.661	1.029	1.596	0.940	0.102	2.107
1.432	1.029	1.191	0.273	0.095	1.191
0.665	1.029	0.809	0.119	0.095	0.809
2.384	0.965	1.596	0.925	0.095	2.107
0.606	0.965	0.809	0.763	0.095	1.917
3.040	0.654	2.107	0.495	0.095	1.596
1.784	0.654	1.596	0.247	0.084	1.191
1.787	0.654	1.596	0.246	0.084	1.191
0.460	0.654	0.809	0.109	0.084	0.809
1.807	0.651	1.596	0.865	0.084	2.107
1.837	0.651	1.596	0.880	0.084	2.107
0.473	0.651	0.809	0.711	0.084	1.917
2.602	0.544	2.107	0.701	0.084	1.917
2.292	0.544	1.917	0.458	0.084	1.596
1.857	0.544	1.763	0.458	0.084	1.596
1.605	0.544	1.596	0.103	0.076	0.809
1.159	0.544	1.409	0.812	0.076	2.107
0.862	0.544	1.191	0.661	0.076	1.917
0.390	0.544	0.809	0.440	0.076	1.596
2.762	0.540	2.107	0.229	0.076	1.191
1.517	0.540	1.596	0.095	0.071	0.809
0.878	0.540	1.191	0.216	0.071	1.191
0.417	0.540	0.809	0.090	0.062	0.809
2.605	0.520	2.107	0.210	0.062	1.191
2.138	0.520	1.917	0.079	0.051	0.809
1.513	0.520	1.596	0.503	0.050	1.917
1.548	0.520	1.596	0.167	0.049	1.191
0.809	0.520	1.191	0.068	0.048	0.809
0.419	0.520	0.809	0.330	0.048	1.596
2.613	0.476	2.107	0.622	0.048	2.107
2.064	0.476	1.917	0.575	0.036	2.107
0.776	0.476	1.191	0.057	0.030	0.809
1.417	0.476	1.596	0.534	0.030	2.107
1.444	0.476	1.596	0.054	0.029	0.809
0.362	0.476	0.809	0.518	0.024	2.107
2.622	0.453	2.107	0.503	0.023	2.107
2.595	0.453	2.107	0.042	0.023	0.809
0.380	0.453	0.809	0.041	0.018	0.809
0.364	0.453	0.809	0.228[a]	0.018	1.596
1.226	0.412	1.596	0.041	0.016	0.809
2.005	0.398	2.049	0.468	0.013	2.107
1.210	0.398	1.596	0.474	0.012	2.107
1.228	0.398	1.596	0.031	0.010	0.809
0.428	0.398	0.947	0.412	0.009	2.107
1.122	0.369	1.596	0.441	0.008	2.107
0.297	0.369	0.809	0.452	0.007	2.107
1.107	0.339	1.596	0.195[a]	0.007	1.596
0.282	0.339	0.809	0.031	0.006	0.809
0.998	0.303	1.596	0.028	0.004	0.809
0.270	0.303	0.809	0.415	0.004	2.107
1.711	0.276	2.107	0.460	0.003	2.107
B. Coexistence curve: liquid					
2.015	0.272	1.633	0.381	0.026	1.614
1.809	0.208	1.630	0.365	0.023	1.614
1.456	0.183	1.629	0.312	0.021	1.613
1.451	0.183	1.629	0.252	0.012	1.611
1.235	0.176	1.628	0.231	0.011	1.611
1.243	0.158	1.627	0.244	0.011	1.611
1.234	0.158	1.627	0.223	0.009	1.610
0.948	0.092	1.623	0.205	0.009	1.610
0.781	0.078	1.621	0.192	0.007	1.609
0.612	0.066	1.620	0.210	0.006	1.608
0.722	0.066	1.620	0.183	0.005	1.608
0.622	0.061	1.620	0.184	0.005	1.608
0.620	0.056	1.619	0.180	0.004	1.607
0.550	0.046	1.618	0.189	0.002	1.606
0.557	0.046	1.618	0.173	0.002	1.605
0.370	0.029	1.615	0.188	0.001	1.604
0.370	0.029	1.615			

TABLE I *(Continued)*

$\Gamma/10^5$ (rad/sec)	ΔT (K)	$q/10^5$ (cm^2/sec)	$\Gamma/10^5$ (rad/sec)	ΔT (K)	$q/10^5$ (cm^2/sec)	$\Gamma/10^5$ (rad/sec)	ΔT (K)	$q/10^5$ (cm^2/sec)	$\Gamma/10^5$ (rad/sec)	ΔT (K)	$q/10^5$ (cm^2/sec)
C. Coexistence curve: vapor						0.793	0.066	1.575	0.207	0.005	1.588
2.487	0.327	1.561	0.300	0.018	1.583	0.725	0.066	1.575	0.198	0.005	1.588
2.229	0.322	1.562	0.307	0.018	1.583	0.580	0.051	1.577	0.197	0.004	1.588
1.931	0.272	1.563	0.275	0.014	1.584	0.647	0.046	1.578	0.194	0.004	1.588
1.656	0.208	1.566	0.271	0.014	1.584	0.518	0.044	1.578	0.188	0.003	1.589
1.476	0.182	1.567	0.238	0.011	1.585	0.455	0.034	1.580	0.193	0.002	1.590
1.187	0.158	1.569	0.223	0.009	1.586	0.415	0.030	1.580	0.189	0.002	1.590
1.062	0.110	1.572	0.217	0.009	1.586	0.412	0.029	1.580	0.198	0.002	1.590
0.948	0.092	1.573	0.201	0.007	1.587	0.386	0.027	1.581	0.190	0.001	1.591
0.955	0.092	1.573	0.203	0.006	1.587	0.352	0.023	1.582	0.189	0.001	1.592
0.803	0.078	1.574	0.203	0.006	1.587	0.352	0.022	1.582			

[a] Obtained with a pulse autocorrelator.

these will be discussed in Sec. III C. The error bars indicate the estimated uncertainty in our values for Γ/q^2 and ΔT.

A few measurements above T_c at $\theta = 90°$ were made with a digital-pulse autocorrelator and are indicated in Fig. 4; all other data were obtained with a spectrum analyzer. The new data, obtained for the second sample using the correlator, agree very well with the older data for $\Delta T \lesssim 2.5$ K but are consistently higher for $\Delta T > 2.5$ K, although the differences are comparable to the experimental uncertainty. It is quite likely that the older data at $\Delta T > 2.5$ K were affected by cell-wall scattering. It was not possible to completely avoid the cell-wall-scattering problem for temperatures greater than about 5 K from the critical temperature. The carbon-dioxide data for large ΔT were likely also affected by the cell-wall-scattering problem, since the same type of cell was used.

In Figs. 4 and 5 the curves are drawn through the data to guide the eye; the linewidth data will be compared with the theoretical predictions in Secs. IV and V. Both for xenon and for CO_2 we find that the measured linewidths are nearly equal for the liquid and vapor phases on the coexistence curve; also we find that in the hydrodynamic region at a given value of ΔT the linewidth measured on the coexistence curve is twice as large as that measured on the critical isochore.

For the values of q used in the present experiments the data for Γ/q^2 are independent of q for $\Delta T \gtrsim 0.1$; in this region we have $q\xi \ll 1$ and the fluid is adequately described by the laws of hydrodynamics, with the thermal diffusivity given by $\chi = \Gamma/q^2$. On the other hand, it is clear from Figs. 4 and 5 that very near the critical point, Γ/q^2 becomes independent of temperature but dependent on q. Note that in order to study this extreme nonhydrodynamic region for these fluids ($q\xi \gg 1$), the light-scattering measurements must be performed at temperatures of the order of 1 mK from T_c.

C. Comparison with Other CO_2 and Xenon Linewidth and Diffusivity Measurements

As mentioned previously, CO_2 is the only fluid for which the diffusivity has been determined in the critical region both by linewidth measurements and by conventional thermodynamic techniques. Although susceptibility data [ρc_p or $(\partial c/\partial \Delta)_{P,T}$] have been obtained for several fluids near T_c, the thermal conductivity has been measured only for CO_2 and the concentration conductivity has not been determined for any mixture in the critical region. Combining Sengers's CO_2 thermal-conductivity data[67] with ρc_p values from the sources discussed in Sec. III D yields for the thermal diffusivity the values plotted on curve (b) of Fig. 5. This calculation differs from the background calculations described later in that here the actual thermal-conductivity values are used, in contrast with values for the background obtained from an analysis of the excess thermal conductivity. The thermodynamic point at $\Delta T = 0.2$ K probably suffers from convection problems, which plague all conventional thermal-conductivity measurements near a critical point. The thermodynamic value at $\Delta T = 1.1$ K is in very good agreement with the light-scattering results, and the systematic departure of the linewidth data from the thermodynamic calculations at higher temperatures is probably due to the cell-wall scattering problem.

Smith and Benedak have measured the linewidth

TABLE II. Rayleigh linewidth Γ for carbon dioxide as a function of the temperature difference ΔT and the magnitude of the scattering vector q.

Γ (10^5 rad/sec)	ΔT (K)	q (10^5 cm^2/sec)	Γ (10^5 rad/sec)	ΔT (K)	q (10^5 cm^2/sec)
A. Critical isochore					
1.137	5.273	0.414	0.044	0.063	0.414
0.999	4.830	0.414	0.691	0.063	1.555
0.876	4.126	0.414	0.660	0.061	1.555
0.757	3.473	0.414	0.660	0.061	1.555
0.710	2.924	0.414	0.547	0.054	1.555
0.591	2.415	0.414	0.512	0.047	1.555
0.548	2.001	0.414	0.432	0.035	1.555
0.456	1.690	0.414	0.446	0.034	1.555
0.425	1.410	0.414	0.427	0.032	1.555
0.371	1.179	0.414	0.415	0.031	1.555
0.325	0.965	0.414	0.419	0.030	1.555
0.282	0.830	0.414	0.440	0.029	1.555
3.761	0.820	1.555	0.402	0.026	1.555
0.270	0.814	0.414	0.408	0.026	1.555
0.202	0.545	0.414	0.410	0.024	1.555
0.155	0.370	0.414	0.383	0.023	1.555
0.157	0.353	0.414	0.361	0.020	1.555
1.979	0.306	1.555	0.396	0.019	1.555
0.134	0.302	0.414	0.339	0.019	1.555
0.113	0.245	0.414	0.349	0.018	1.555
0.112	0.245	0.414	0.361	0.016	1.555
1.574	0.245	1.555	0.338	0.016	1.555
1.599	0.239	1.555	0.365	0.014	1.555
0.095	0.198	0.414	0.355	0.011	1.555
0.092	0.198	0.414	0.336	0.011	1.555
1.367	0.196	1.555	0.324	0.011	1.555
1.140	0.168	1.555	0.328	0.010	1.555
1.147	0.163	1.555	0.325	0.008	1.555
0.084	0.154	0.414	0.286	0.007	1.555
1.068	0.136	1.555	0.291	0.006	1.555
0.071	0.129	0.414	0.309	0.006	1.555
0.867	0.113	1.555	0.308	0.006	1.555
0.880	0.111	1.555	0.308	0.006	1.555
0.880	0.099	1.555	0.308	0.006	1.555
0.060	0.094	0.414	0.308	0.006	1.555
0.060	0.094	0.414	0.308	0.006	1.555
0.060	0.093	0.414	0.308	0.006	1.555
0.644	0.071	1.555	0.308	0.006	1.555
0.045	0.068	0.414	0.308	0.006	1.555
B. Coexistence curve: liquid					
2.450	0.192	1.577	1.539	0.089	1.572
2.626	0.185	1.577	1.354	0.076	1.571
1.963	0.151	1.575	1.049	0.067	1.570
2.042	0.143	1.575	1.250	0.057	1.569
2.067	0.125	1.574	0.817	0.046	1.568
1.571	0.106	1.573	0.983	0.044	1.568
1.539	0.105	1.573	0.974	0.037	1.567
1.587	0.104	1.573	0.543	0.027	1.566
1.590	0.102	1.573	0.500	0.018	1.564
1.674	0.101	1.573	0.402	0.014	1.563
1.508	0.096	1.572	0.408	0.008	1.561
1.420	0.089	1.572			
C. Coexistence curve: vapor					
2.853	0.192	1.530	1.634	0.089	1.536
2.937	0.185	1.531	1.769	0.089	1.536
2.199	0.151	1.532	1.458	0.076	1.537
2.450	0.143	1.532	1.238	0.067	1.537
2.331	0.125	1.533	1.455	0.057	1.538
1.797	0.106	1.535	0.974	0.046	1.539
1.766	0.105	1.535	1.169	0.044	1.540
1.876	0.104	1.535	1.144	0.037	1.540
1.816	0.102	1.535	0.679	0.027	1.542
1.901	0.101	1.535	0.556	0.018	1.543
1.674	0.096	1.535			

for xenon along both sides of the coexistence curve in the hydrodynamic region ($0.026 \leq \Delta T \leq 0.9$ K) at a scattering angle of $\theta = 26°$; in addition, the linewidth was determined at several angles at $\Delta T = 0.006$ in the vapor phase.[8,9] The Smith and Benedek data are in very good agreement with our data; a few representative points of their data are plotted in Fig. 4(a).

Maccabee and White[7] have reported linewidth measurements along the critical isochore in the hydrodynamic region of CO_2, and they found their values to be in agreement with ours. A few representative points taken from Fig. 1 of Maccabee and White are shown in Fig. 5(b).

D. Auxiliary Data

The parameters required for a comparison of the linewidth data with the predictions of the mode-mode-coupling and decoupled-mode theories are listed in Table III: the critical point is specified in Sec. III A; the parameters needed to calculate the linewidth background are given in Table III B–III F; and the parameters needed to calculate the critical part of the linewidth are given in Sec. III G–III J.

The critical-point parameters tabulated in Table III A are taken from Refs. 64, 65, 68, 69, 70, 73, 74, 75, and 80. References 64, 68, 69, and 70 were also used for the refractive index below T_c, needed in order to calculate q along the coexistence curve.

The constant-pressure specific heat was determined using the thermodynamic relation

$$\rho c_p = \rho c_v + T\left(\frac{\partial P}{\partial T}\right)_\rho^2 \kappa_T, \tag{31}$$

where κ_T is the isothermal compressibility. The pressure derivative $(\partial P/\partial T)_\rho$ varies slowly along the critical isochore but varies rapidly as the critical point is approached from below T_c in either the liquid or vapor phase. Below T_c, $(\partial P/\partial T)_\rho$ was determined for each phase from its relation to the vapor-pressure derivative $(\partial P/\partial T)_{cx}$ [31]:

$$\left(\frac{\partial P}{\partial T}\right)_\rho = \left(\frac{\partial P}{\partial T}\right)_{cx} - \frac{1}{\rho K_T}\left(\frac{\partial \rho}{\partial T}\right)_{cx}, \tag{32}$$

where the cx subscript indicates the coexistence curve.

We assume that the isothermal compressibility is described by the critical part alone in the temperature region of interest:

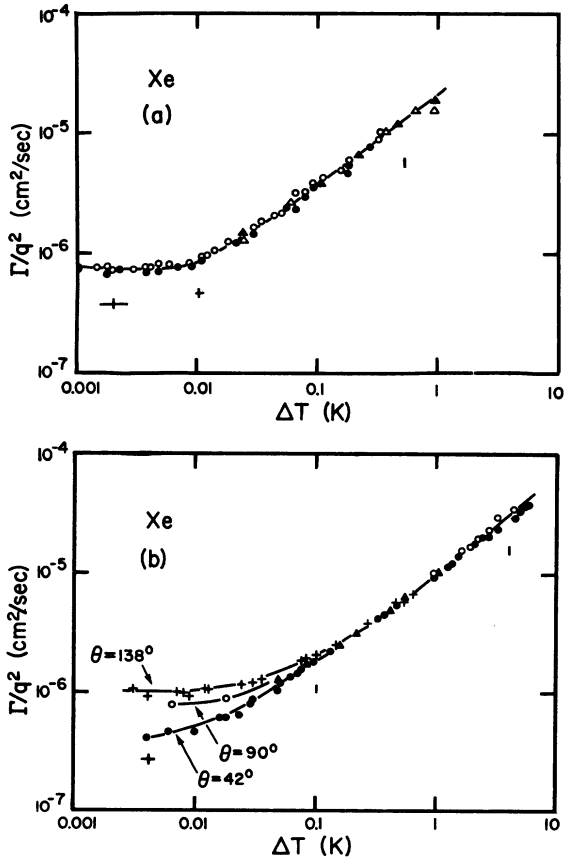

FIG. 4. Γ/q^2 as a function of ΔT for xenon. The linewidth Γ is the measured value with no background subtractions. (a) Coexistence curve: ●, ○, $\theta = 90°$, data of Lim and Swinney (Refs. 8 and 10); ▲, △, $\theta = 22.4°$, data of Smith and Benedek (Refs. 8 and 9). An open symbol represents the vapor phase and a closed symbol the liquid phase. (b) Critical isochore: +, $\theta = 138°$; ●, $\theta = 42°$; ▲, $\theta = 90°$; ○, $\theta = 90°$, data obtained by Lim (Ref. 10) using a pulse correlator. The error bars represent the uncertainties in Γ/q^2 and ΔT at extreme and intermediate values of ΔT.

$$\kappa_T = (\Gamma_T/P_c)\,\epsilon^{-\gamma} \tag{33}$$

along the critical isochore, and

$$(\rho/\rho_c)^2\,\kappa_T = (\Gamma'_T/P_c)\,\epsilon^{-\gamma} \tag{34}$$

along both sides of the coexistence curve, where the exponent γ is assumed to be the same for the three paths, as theory and experiment indicate.

For CO_2 the results of Levelt Sengers and Chen[74] were used for $(\partial P/\partial T)_\rho$ $[T > T_c]$ and $(\partial P/\partial T)_{cx}$ $[T < T_c]$. Those authors fit their high-precision pressure-temperature data from the critical isochore and the coexistence curve to a form of the extended scaling-law equation of Green, Cooper, and Levelt Sengers,[76]

$$(P - P_c)/P_c = c_1\epsilon + P_1^{\pm}\epsilon^{2-\alpha} + \rho_c H_2^{\pm}\epsilon^{3-2\alpha-2\beta}, \tag{35}$$

where the + and − superscripts indicate the critical isochore and the coexistence curve, respectively. The parameters in (35) determined by Levelt Sengers and Chen (Table X of Ref. 74) are given in Table III B.

For xenon on the critical isochore we obtained $(\partial P/\partial T)_\rho$ from a least-squares fit of the pressure-

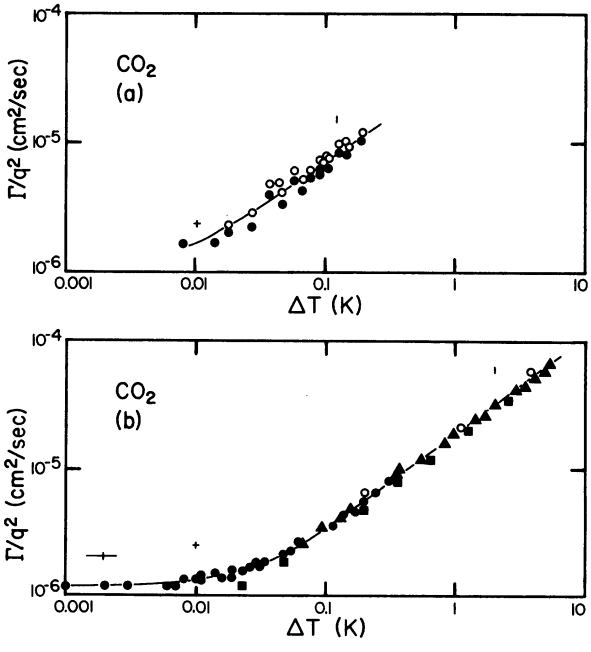

FIG. 5. Γ/q^2 as a function of ΔT for CO_2. The linewidth Γ is the measured value with no background subtractions. (a) Coexistence curve: ●, $\theta = 90°$ (liquid); ○, $\theta = 90°$ (vapor). (b) Critical isochore: ●, $\theta = 90°$; ▲, $\theta = 21.8°$; ■, data of Maccabee and White (Ref. 82); ○, thermodynamic values of $\lambda q^2/\rho c_p$ [see Sengers (Ref. 67) and text]. The error bars represent the uncertainties in Γ/q^2 and ΔT.

TABLE III. Parameters from other experiments used in the analysis of the xenon and carbon dioxide linewidth data. Reference numbers are given in parentheses.

Parameter	Xenon		Carbon dioxide	
A. Critical-point parameters				
P_c	58.402×10^6 dyne cm^{-2}	(73)	73.860×10^6 dyne cm^{-2}	(74)
ρ_c	1.11 g cm^{-3}	(65, 73)	0.464 g cm^{-3}	(74, 75)
T_c	289.757 K	(80)	304.18 K	(74)
n_c (λ_0=6328 Å)	1.136 65	(64, 68)	1.1074	(69, 70)
B. Pressure-temperature relation on the critical isochore [Eq. (35)]				
α	0.08	(73, 77, present analysis)	0.09	(74)
β	0.35	(75)	0.35	(74)
C_1	5.925 384	(73, 77, present analysis)	6.992 153	(74)
P_1^+	2.635 562	(73, 77, present analysis)	6.561 674	(74)
P_1^-	...	(See text)	24.857 95	(74)
$\rho_c H_2^+$	−2.616 886	(73, 77, present analysis)	−8.489 391	(74)
$\rho_c H_2^-$	...	(See text)	−16.739 76	(74)
std. dev.	5.4×10^{-3}%	(Present analysis)	1.8×10^{-3}%	(74)
C. Compressibility [Eqs. (33) and (34)]				
Γ_T	0.067 78	(80)	0.0573	(81)
Γ_T'	0.016 40	(80)	0.013 64	(81, 75, see text)
γ	1.21	(80)	1.219	(81)
D. Constant-volume specific heat on the critical isochore [units: 10^6 erg cm^{-3} K^{-1}]				
$\rho_c c_v$	$[2.2922\epsilon^{-0.146}-1.6928]$	(83–85)	$-[0.0973+1.458\ln\epsilon]$	(87)
E. Dilute-gas thermal conductivity near T_c [units: erg cm^{-1} sec^{-1} K^{-1}]				
$\lambda(0,T)$	$[1614+522\epsilon]$	(92, 93)	$[4353+2521\epsilon]$	(94)
F. Excess thermal conductivity: $\tilde{\lambda}(\rho)=\lambda_1\rho+\lambda^2\rho^2+\lambda_3\rho^3+\lambda_4\rho^4$ [$\tilde{\lambda}$ in erg cm^{-1} sec^{-1} K^{-1} and ρ in g cm^{-3}]				
λ_1	590.5	(62, 96)	3411	(62, 95)
λ_2	381.7	(62, 96)	2825	(62, 95)
λ_3	−107.0	(62, 96)	4876	(62, 95)
λ_4	59.04	(62, 96)	0	(62, 95)
G. Shear vicosity on the critical isochore: $\eta_s=\eta_s^C+\eta_s^B$ [units: μP]				
η_s^C	$-[16.35\ln\epsilon+68.66]$	(60)	(a) $\eta_s^C/\bar{\eta}_s=-[0.034\,18\ln\epsilon+0.1519]$ (b) $\eta_s^C=-[23\ln\epsilon+164]$	(See text) (60, 99, 100, see text)
η_s^B	$[525+219\epsilon]$	(60)	$[327+125\epsilon]$	(60, 100)
H. Dilute-gas shear viscosity near T_c [units: μP]				
$\eta_s(0,T)$	$[247+219\epsilon]$	(98)	$[152+125\epsilon]$	(100)
I. Excess shear viscosity: $\tilde{\eta}_s(\rho)=\eta_1\rho+\eta_2\rho^2+\eta_3\rho^3+\eta_4\rho^4$ [$\tilde{\eta}$ in μP and ρ in g cm^{-3}]				
η_1	35.96	(97, 98)	42.58	(100)
η_2	415.78	(97, 98)	661.70	(100)
η_3	−337.56	(97, 98)	82.89	(100)
η_4	123.68	(97, 98)	0	(100)

TABLE III *(Continued)*

Parameter	Xenon		Carbon dioxide	
J. Correlation length				
ξ_0	2 Å	(80)	1.50 Å	(81)
ξ_0'	1 Å	(79)	0.714 Å	(81, see text)
ν	0.63	(8, 9)	0.633	(81)

temperature data of Habgood and Schneider[73] (eight points, $0 \leq \Delta T \leq 1.8$ K) and Michels *et al.*[77] (four points, $8.4 \leq \Delta T \leq 33.4$ K) to Eq. (35), and the results of this analysis are shown in Table III B. The results of the vapor-pressure measurements of Theeuves and Bearman [Eq. (1), Ref. 78] were used for $(\partial P/\partial T)_{cx}$ for xenon.

The slope of the coexistence curve $(\partial\rho/\partial T)_{cx}$ was obtained for CO_2 from Vicentini-Missoni *et al.*[75] and for xenon from Garside *et al.*[64]

Vicentini-Missoni, Levelt Sengers, and Green[75] have reported values of γ, Γ_T, and Γ_T' for xenon determined from a scaling-law equation-of-state analysis of the PVT data of Habgood and Schneider.[73] They found $\gamma = 1.26$, $\Gamma_T = 0.05870$, and $\Gamma_T' = 0.0143$, while Smith, Giglio, and Benedek[79,80] found that measurements of the absolute scattering intensity yielded $\gamma = 1.21$, $\Gamma_T = 0.6778$, and $\Gamma_T' = 0.01640$. Although the temperature dependence of the *relative* scattering intensity can be accurately measured to obtain the exponent γ, the determination of the coefficients Γ_T and Γ_T' requires an *absolute* measurement of the scattering intensity, which is quite difficult. Therefore, the values of Γ_T and Γ_T' are probably best obtained from the PVT data. We have repeated the PVT analysis of Vicentini-Missoni *et al.*,[75] with γ fixed at 1.21 and have obtained $\Gamma_T = 0.07325$ and $\Gamma_T' = 0.01779$, about 8% and 8.5%, respectively, higher than the values found by Smith, Giglio, and Benedek.[79,80] The parameters γ and Γ_T for CO_2, determined by Lunacek and Cannell[81] from extensive turbidity measurements, are given in Table III C. (White and Maccabee[82] have also determined γ for CO_2 from measurements of the scattering intensity.) The value of Γ_T' for CO_2 (cf. Table III C) was obtained by combining Γ_T with the Γ_T/Γ_T' ratio reported by Vicentini-Missoni *et al.*[75]

The xenon c_v data of Edwards *et al.*,[83] which are uncertain by ±3 J/mole K in absolute value, were decreased by 2 J/mole K to agree with the data of Schmidt *et al.*,[84] Habgood and Schneider,[85] and Michels *et al.*[77] Combining these four sets of data then yields for c_v on the critical isochore of xenon the result given in Table III D. For the critical isochore of CO_2 the data of Lipa *et al.*[86] have a ±10 J/mole K (≃6%) uncertainty; therefore, we have used the c_v values derived by Feke, Fritsch, and Carome[87] from their low-frequency (≃1 kHz) sound-velocity data.

Equation (31) together with the relation between the specific heats and low-frequency velocity, $u^2 = c_p/(\rho c_v \kappa_T)$, yields

$$\rho c_v = T(\partial P/\partial T)_\rho^2 \kappa_T/(\rho u^2 \kappa_T - 1). \tag{36}$$

Sound velocities determined in ultrasonic experiments were substituted into (36) to calculate ρc_v along the two sides of the coexistence curve; the data of Mueller *et al.*[88] were used for xenon and the data of Herget,[89] Parbrook and Richardson,[90] and Tielsch and Tanneberger[91] were used for CO_2. For both fluids the contribution of the ρc_v to ρc_p in (31) is less than 3% in the temperature range of our linewidth data below T_c; hence high accuracy is not required for the ρc_v values used below T_c, so these are not included in Table III.

The separation of c_p into critical background parts is somewhat ambiguous. We have calculated c_p^C in two different ways for xenon on the critical isochore: (i) using the expression suggested by Sengers,[62]

$$c_p^C = c_p - c_v, \tag{37}$$

and (ii) using

$$c_p^C = \lim_{T \to T_c} (c_p) = (P_c c_1^2/\rho_c T_c)\Gamma_T \epsilon^{-\gamma}, \tag{38}$$

which follows from (31), (33), and (35). The difference between c_p^C calculated from (37) and (38) is insignificant in the temperature range of our data, as Table IV illustrates. In addition, Table IV shows that c_p^C/c_p differs from unity by at most a few percent.

The background thermal conductivity is given by the sum of two terms [Eq. (6)]: the dilute gas thermal conductivity, given in Table III E,[92-94] and the excess thermal conductivity, tabulated in Table III F.[62] The excess thermal conductivity was obtained by Sengers[62] from an analysis of the data of Le Neindre *et al.*[95] for CO_2 and the data of Tufeu[96] for xenon.

Recently Strumpf, Collings, and Pings[60] have completed extensive measurements of the shear viscosity of xenon as a function of temperature along 10 isochores near the critical isochore. These data, obtained from measurements of the

damping of a torsionally oscillating quartz cylinder, show a small increase in the viscosity very near the critical point (e.g., 17% at $\Delta T = 0.02$ and $\rho = \rho_c$). For $\Delta T \gtrsim 2$ K, the viscosity values of Strumpf *et al.* are in reasonable agreement with the values calculated for the background viscosity using the data of Reynes and Thodos[97] and Dawe and Smith.[98]

The result for the viscosity of xenon obtained by Strumpf *et al.* for the critical isochore is given in Table III G. The data for the nine near-critical isochores studied by Strumpf *et al.* were extrapolated to the coexistence curve to obtain the viscosity values along this path that we used in our linewidth-data analysis; however, since the extrapolated viscosities differ from the background viscosity by only a few percent (e.g., 16% at $T = 0.01$ K for either side of the coexistence curve), we give in Table III only the background viscosity for the coexistence curve $[\eta_s^B(\rho, T) = \tilde{\eta}_s(\rho) + \eta_s(0, T)$; see parts H and I of Table III].

For CO_2 the background viscosity $\eta_s^B(\rho, T)$ is accurately known from the extensive measurements that have been performed outside of the critical region[99,100]; the results for $\eta_s(0, T)$ and $\tilde{\eta}_s(\rho)$ are listed in Table III, parts H and I, respectively. In the critical region, however, there have been few measurements of the viscosity of CO_2, so we have supplemented those few data with estimates of the critical part of the viscosity based on the results obtained for other systems. As will be shown in Sec. V, the ratio $\eta_s^C/\tilde{\eta}_s$ is nearly the same for all those systems for which extensive measurements have been made. We have taken an average value for this ratio [which is given in Table III G(a)] to use in estimating η_s^C for CO_2, and the results are in reasonable agreement with the values obtained from an extrapolation of the available CO_2 viscosity data [Table III G(b)].[60,99] Since η_s^C is only a small fraction of the total viscosity in the region of interest, the uncertainty in Γ^* from this estimation should be small.

TABLE IV. A comparison of the critical part of the specific heat (c_ρ^C) with the full specific heat (c_ρ), with c_ρ^C calculated in two different ways: (i) $c_\rho^C = c_\rho - c_v$, and (ii) $c_\rho^C = \lim_{T \to T_c} c_\rho = (P_c c_1^2/\rho_c T_c)\Gamma_T \epsilon^{-\gamma}$.

	Xenon			Carbon dioxide		
ΔT (K)	c_ρ^C(10^8 erg/g K) (i)	(ii)	$\left(\frac{c_\rho^C \text{(ii)}}{c_\rho}\right)$	c_ρ^C(10^8 erg/g K) (i)	(ii)	$\left(\frac{c_\rho^C \text{(ii)}}{c_\rho}\right)$
5.000	0.0635	0.660	0.935	2.12	2.15	0.935
1.000	4.45	4.49	0.984	15.05	15.16	0.983
0.500	10.30	10.35	0.992	35.0	35.2	0.991
0.050	167	167	0.999	580	580	0.999
0.005	2710	2710	1.000	9600	9600	1.000

Independent measurements of the correlation length have been performed for xenon by Smith, Giglio, and Benedek[9,80] for $T > T_c$ and by Giglio and Benedek[79] for $T < T_c$. In CO_2 Lunacek and Cannell[81] have measured ξ along the critical isochore (see also White and Maccabee[82]). Below T_c we have calculated ξ for CO_2 from the Ornstein-Zernike relation[79]

$$\xi^2 = \rho_n k_B T R^2 K_T, \tag{39}$$

where ρ_n is the number density and R is the direct correlation length; it was assumed that R has the same value below T_c as along the critical isochore. The correlation-length parameters for xenon and CO_2 are listed in Table III J, where ξ_0 and ξ_0' are the correlation-length coefficients above and below T_c, respectively.

IV. COMPARISON OF EXPERIMENTS WITH MODE-MODE COUPLING THEORY

A. Carbon Dioxide

We now compare the measured linewidths with the theoretical expression for the total linewidth [Eq. (11)] evaluated using the mode-mode-coupling-theory result [Eq. (24)] for Γ^C.

The data for Γ/q^2 for carbon dioxide on the critical isochore are plotted as a function of ΔT in Fig. 6. Included in Fig. 6 are theoretical curves

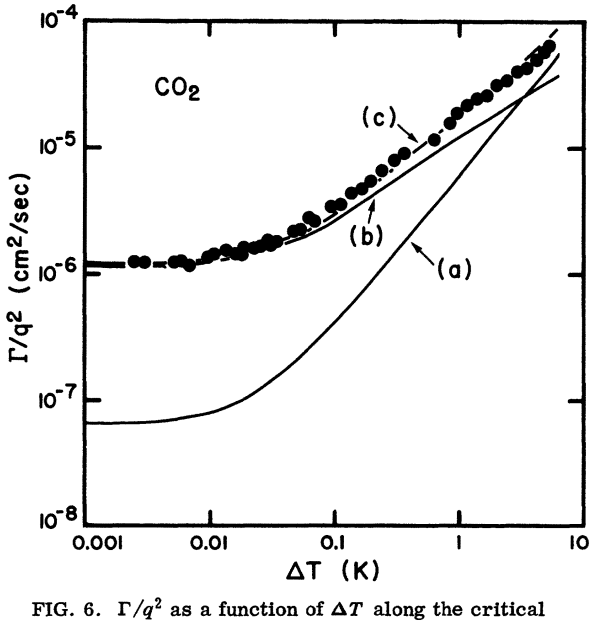

FIG. 6. Γ/q^2 as a function of ΔT along the critical isochore of CO_2. The theoretical curves represent (for $\theta = 90°$): (a) the background contribution; (b) the contribution of the critical part of the linewidth ($\Gamma^C c_\rho^C/q^2 c_\rho$), calculated using the mode-mode-coupling theory; (c) the sum of the critical and background contributions. The symbols represent the measured values of Γ/q^2.

showing the total linewidth [curve (c)] and the separate contributions of the background part [curve (a)],

$$(\Gamma/q^2)^B = (\lambda^B/\rho c_p)(1+q^2\xi^2), \tag{40}$$

and the critical part [curve (b)],

$$\left(\frac{\Gamma}{q^2}\right)^C = \left(\frac{c_p^C}{c_p}\right)\left(\frac{\Gamma^C}{q^2}\right) = \left(\frac{c_p^C}{c_p}\right)\frac{k_B T}{6\pi\eta_s \xi^3 q^2} K_0(q\xi)H(q\xi). \tag{41}$$

[See Eqs. (11) and (24).] The evaluation of the theoretical expressions (40) and (41) involves no adjustable parameters, all parameters having been obtained from independent measurements (Table III). As can be seen, the data are in good agreement with the theory.

Note that the background contribution is large at temperatures several degrees above T_c, amounting to one-half the total linewidth at $\Delta T \simeq 3.5$ K. The background and critical parts of the linewidth are both proportional to q^2 in the hydrodynamic region, but in the extreme nonhydrodynamic region ($q\xi >> 1$), where the background and critical parts both become independent of temperature, the two contributions have a different q dependence: $\Gamma^B \propto q^4$ and $\Gamma^C \propto q^3$. Thus in the $q\xi >> 1$ limit, the background contribution is negligible for sufficiently small angles. The data in the $q\xi >> 1$ region in Fig. 6 were obtained at a scattering angle of 90°; for these data the background contribution is 6% of the total linewidth.

The background contribution to the linewidth is even larger for xenon and SF_6 than it is for CO_2; for example, for these three fluids on the critical isochore at $\epsilon = 10^{-2}$, the ratio Γ^B/Γ^C is 0.87 for CO_2, 1.00 for xenon, and 2.1 for SF_6. Nevertheless, as we shall show for xenon and SF_6 as well as for CO_2, when the background contribution is subtracted from the linewidths measured for these fluids, the resultant values for the critical part of the linewidth are in reasonably good agreement with the theory. This agreement supports the form assumed for the background contribution [see Eq. (11)], which is based on the Sengers-Keyes ansatz[30] for the thermal conductivity background [Eq. (6)] and our assumption[6,35] that c_p can be separated into background and critical parts, with the q dependence of c_p given in Eq. (8).

We have included Fig. 6 to show the separate contributions of the background and critical parts of the linewidth (similar plots have been previously presented for xenon[8,80] and for SF_6[35,36]). However, as discussed in Sec. II F, in comparing linewidth data with the mode-mode-coupling theory, it is more appropriate to consider dimensionless plots of the scaled linewidth Γ^* [Eq. (30)] as a function of $q\xi$; hence our subsequent graphs will be of this form. Such a plot is shown for CO_2 in Fig. 7(a), which includes data along the coexistence curve as well as the data for the critical isochore. The deviation of the measured linewidths on the critical isochore from the theoretical values for the total linewidth is shown in Fig. 7(b).

The measured linewidth values in the far hydrodynamic region ($q\xi \lesssim 0.02$) are systematically smaller than the theoretical linewidths. This departure from the theory, which has been previously noted for xenon[8,80] and SF_6,[36] can probably be explained by the sample cell-wall-scattering problem discussed in Sec. III A.

The uncertainty in $\Gamma^* \equiv (6\pi\eta_s\Gamma^C/k_B T q^3)$ and in $q\xi$ is indicated for the data on the critical isochore by the error bars in Fig. 7(a). The uncertainty in the value of the total linewidth at any temperature within the range of the measurements is only a few percent; however, the uncertainty in the *scaled linewidth* Γ^* increases with increasing ΔT for CO_2, and for other pure fluids as well,

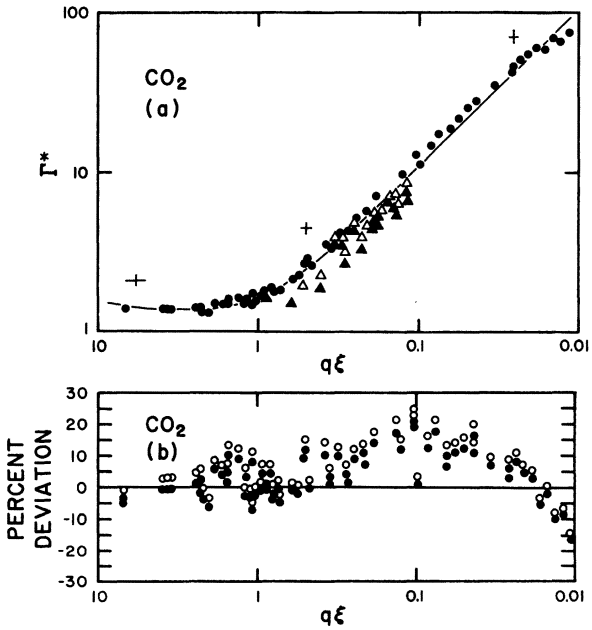

FIG. 7. (a) Γ^* as a function of $q\xi$ for CO_2. The curve represents the mode-mode-coupling theory with all modifications. The error bars represent the uncertainties in Γ^* and $q\xi$ at extreme and intermediate values of $q\xi$. ●, critical isochore; ▲, coexistence curve (liquid); △, coexistence curve (vapor). (b) Percent deviation of the *measured* linewidths on the critical isochore from the theoretical values for the *total* linewidth. ●, with all corrections to the theory; ○, with vertex and correlation-function corrections omitted.

because of the increasing importance of the background term which must be subtracted from the measured linewidths to obtain the quantity Γ^C, which is used in calculating Γ^*. In the region where $q\xi \gtrsim 2$ the uncertainty in Γ^* is primarily due to the uncertainty in the values of the macroscopic shear viscosity η_s very near T_c (see Sec. III D). In this region the uncertainty in $q\xi$ arises primarily from the uncertainty in ΔT at the temperatures of these measurements, a few millidegrees from T_c; far from T_c the uncertainty in $q\xi$ is primarily due to the reported uncertainty of the measured values of the correlation length.

Below T_c the uncertainty in the measured linewidths is larger and the background contribution to the linewidth is more important than for the data above T_c; also, the shear viscosity, which is strongly density dependent, is not as well known along the coexistence curve as it is along the critical isochore. Moreover, since ξ has not been directly measured below T_c, we have had to deduce values of ξ along the coexistence curve from the values measured for the critical isochore. For the reasons just stated the uncertainties in Γ^* and $q\xi$ are much larger below T_c than above T_c; hence the data for $T < T_c$ are not included in Fig. 7(b) even though those data agree with the theory within the experimental uncertainty.

Figure 7(b) shows the deviation of the linewidth data from the theory for two cases: (i) when the modifications to the mode-mode-coupling theory considered in Sec. III F are included, in which case the rms difference between theory and experiment is 10.6%, and (ii) when the vertex and correlation-function corrections are omitted, in which case the rms difference between theory and experiment is 12.7%. The vertex and correlation-function corrections are not more than 5% (cf. Fig. 1), which is less than the rms difference between theory and experiment. More-accurate measurements of both the linewidth and the parameters which enter the theory are required before definitive conclusions can be drawn concerning the vertex- and correlation-function modifications.

B. Xenon

Figure 8(a) is a plot of Γ^* as a function of $q\xi$ for all our xenon data, with the curve again representing the mode-mode-coupling theory with corrections and the error bars indicating the un-

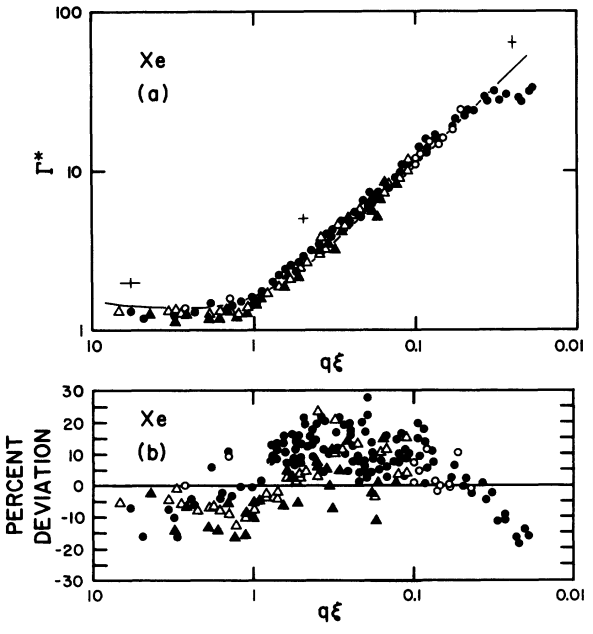

FIG. 8. (a) Γ^* as a function of $q\xi$ for xenon (with parameters taken from Table III). The curve represents the mode-mode-coupling theory with all modifications, and the error bars represent the uncertainties in Γ^* and $q\xi$ at extreme and intermediate values of $q\xi$. (b) Percent deviation of the *measured* linewidths from the theoretical values for the *total* linewidth. Critical isochore: ●, data obtained with a spectrum analyzer; ○, data obtained with a pulse autocorrelator. Coexistence curve: ▲, liquid; △, vapor.

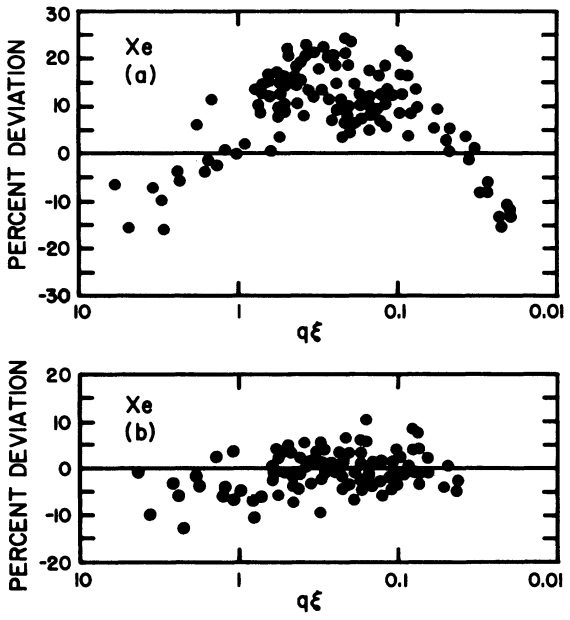

FIG. 9. Percent deviation of the measured linewidths from the theoretical values for the total linewidth for xenon on the critical isochore, with the compressibility coefficient given by $\Gamma_T = 0.073\,25$, as determined from an analysis of PVT data (Ref. 73). (a) $\xi = 2.0\epsilon^{-0.63}$ Å, measured by Smith (Ref. 9). (b) $\xi = 2.32\epsilon^{-0.58}$ Å, obtained by fitting the theoretical curve to the data (excluding those data for which $q\xi \lesssim 0.03$) with the correlation-length coefficient ξ_0 and exponent ν allowed to vary freely.

certainties in Γ^* and $q\xi$ for the data on the critical isochore. This comparison with the theory, like that in Figs. 6 and 7, involves no adjustable parameters, all quantities having been determined in independent experiments (cf. Table III). The agreement between the measured linewidths and the theoretical values for the total linewidth is reasonably good, as the deviation plot in Fig. 8(b) shows. However, although the linewidths measured for the extreme nonhydrodynamic region above T_c and along the two sides of the coexistence curve below T_c agree with the theory within the experimental uncertainty, our most extensive xenon linewidth data are in the hydrodynamic region above T_c, and these linewidths are systematically higher than the theoretical linewidths by about 14% (except for the data corresponding to $q\xi \lesssim 0.03$, which subsequent measurements have shown to be affected by the cell-wall-scattering problem—see Sec. III A).

We have considered all sources of error in the measured linewidths and in the parameters which enter the theory to determine whether or not the 14% difference between theory and experiment, observed only for the data in the hydrodynamic region on the critical isochore, is significant. The major sources of error are the errors in c_p, λ^B, Γ, ξ, and η_s; we now consider the uncertainties in each of these quantities.

The uncertainty in c_p arises primarily from the uncertainty in the compressibility coefficients Γ_T and Γ_T'. As discussed in Sec. III D, our analysis of the Habgood and Schneider PVT data yields values for the compressibility coefficients which are 8% larger than those of Smith *et al.*[80] The data for the critical isochore in Fig. 8, analyzed using the Smith *et al.* value for Γ_T, were reanalyzed using the value of Γ_T deduced from the PVT data, and Fig. 9(a) shows the deviation of the measured linewidths from the resultant theoretical values of the total linewidth. For the data in Fig. 8 the rms difference between theory and experiment for the data on the critical isochore is 14%, while in Fig. 9(a) the corresponding number is 15%; hence an 8% change in c_p changes the rms difference between theory and experiment by only 1%.

The background thermal conductivity is essentially constant on the critical isochore; therefore, an error in this quantity would introduce a temperature-dependent error in the background term in the linewidth [Eq. (40)]. The estimated uncertainty in the *total* theoretical linewidth due to the uncertainty in Γ^B varies from 1.0% for $q\xi = 0.8$ to 3.5% for $q\xi = 0.05$.

The uncertainty in our measured average values for the total linewidth is 3%; the scatter in the individual data points is of course larger. Our values for the linewidth are corroborated by the measurements of Smith and Benedek,[8,9] who obtained values for the linewidth which agree with ours well within the combined uncertainty (8%) of the two experiments.

The critical part of the linewidth is inversely proportional to the viscosity, so uncertainties in the viscosity are an especially important contribution to the uncertainty in Γ^* near T_c. The xenon viscosity data of Strumpf *et al.*[60] exhibit a critical behavior similar to that observed for the viscosity of other systems (see Sec. V A), and far from the critical point the Strumpf *et al.* viscosity data are corroborated by the independent measurements of Reynes and Thodos.[97] The estimated uncertainty in the values for the viscosity is 3%.[60]

In comparison of the linewidth data with the theory, the primary source of uncertainty in the independent variable $q\xi$ is the uncertainty in ξ. The uncertainty in the correlation lengths measured by Smith, Giglio, and Benedek is 5%.[9] In order to see if slightly different values for the correlation length could bring the theory and experiment into agreement, we have fit the linewidths to the theory using a nonlinear least-squares fitting routine in which the correlation length parameters ν and ξ_0 were allowed to vary freely. (Since the linewidths at high temperatures are known to be affected by the cell-wall-scattering problem, those data are not included in this and other least-squares analyses of the data.) The best fit was achieved with $\nu = 0.58$ and $\xi_0 = 2.32$ Å, with an rms difference between theory and experiment of 4.6%. The percent difference between theory and experiment is shown as a

TABLE V. Results obtained from a nonlinear least-squares fitting of the mode-mode-coupling theory (including the modifications in Fig. 1) to the linewidth data for xenon, with the correlation-length exponent ν fixed at different values and the coefficient ξ_0 allowed to vary freely. The third column shows the rms deviation between theory and experiment for different values of ν with the best-fit values of ξ_0. Data for which $q\xi \lesssim 0.03$ were omitted from the analysis, since they were affected by the cell-wall-scattering problem.

ν	ξ_0 (Å)	rms deviation (%)
0.53	3.40	6.1
0.55	2.93	5.2
0.58	2.32	4.6
0.60	2.06	4.8
0.62	1.79	5.5
0.63	1.67	5.9

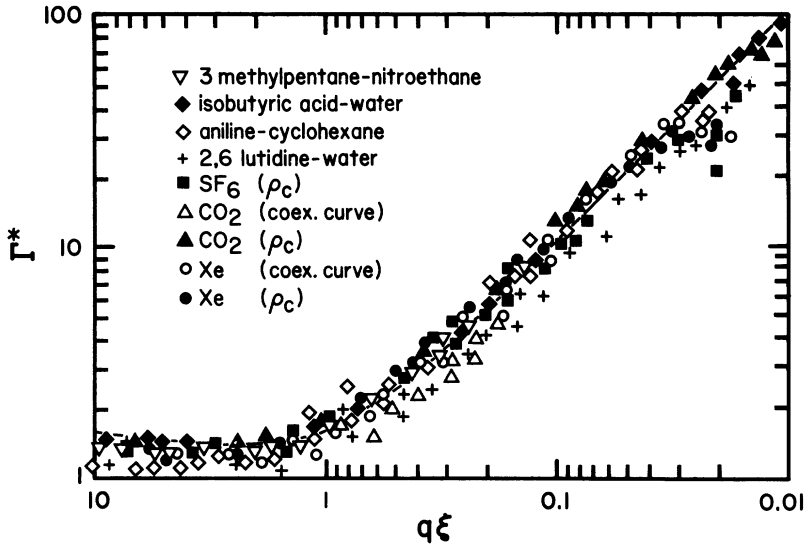

FIG. 10. Γ^* as a function of $q\xi$ for several systems. The curve represents the mode-mode-coupling theory including the modifications in Fig. 1. Background subtractions have been made for only the pure fluids. ◆, isobutyric acid water; ▽, 3 methylpentane-nitroethane; +, 2,6 lutidine-water; ◇, aniline-cyclohexane; ■, SF_6; ●, xenon, critical isochore; ○, xenon, coexistence curve; ▲, CO_2, critical isochore; △, CO_2, coexistence curve.

function of $q\xi$ in Fig. 9(b).

In another least-squares analysis of the same data, the exponent ν was fixed at different values and ξ_0 was allowed to vary freely to achieve the best fit of the scaled linewidths to the theory; the results of this analysis are presented in Table V. The linewidth data are fairly insensitive to the value of the exponent ν as Table V illustrates; the rms difference between theory and experiment increases from 4.6% to 6.0% as ν changes by ± 0.05 from the value which gives the best fit, $\nu = 0.58$. The values of ν and ξ_0 are highly correlated; although ξ_0 varies considerably as ν increases from 0.53 to 0.63, the actual variation of the correlation length ξ (at a fixed temperature) is much smaller for the temperature range of our data.

Our best fit value of ξ_0 corresponding to $\nu = 0.63$ is 1.67 Å, which is 16% smaller than the value (2 Å) obtained by Smith *et al.*[101] for the same ν. Smith *et al.* give an uncertainty in their values of ξ of only 5%, considerably less than the 16% change required in order to bring the data into agreement with the theory.

We conclude, finally, that the 14% difference between theory and experiment for the xenon linewidth data on the critical isochore in the hydrodynamic region is slightly greater than the combined stated uncertainties in our linewidth data and in the parameters which enter the theory; however, this difference may not be significant because any one of the several quantities used in calculating the linewidth or $q\xi$ could be in error by an amount slightly larger than the reported uncertainties. Clearly more viscosity, correlation-length, and linewidth measurements are needed.

C. Other Fluids

There are five other fluid systems for which all quantities in Eq. (30) have been directly determined or can be accurately estimated: SF_6,[35,36] isobutyric acid-water,[61] 3 methylpentane-nitroethane,[23,24] 2, 6 lutidine-water,[57] and aniline-cyclohexane.[18,19] Figure 10 is a plot of Γ^* as a function of $q\xi$ for these systems and for xenon

TABLE VI. Values for the ratio of the background viscosity at the critical point $\eta_s^B(\rho_c, T_c)$ to the dilute-gas viscosity at the critical temperature $\eta_s(0, T_c)$, for several single component fluids. Background viscosities were calculated from values for the excess viscosities.

Fluid	$\frac{\eta_s^B(\rho_c, T_c)}{\eta_s(0, T_c)}$	Reference
Xe	2.34	(60, 97, 98)
CO_2	2.22	(99, 100)
Ar	2.34	(102)
Kr	2.34	(97, 98)
N_2	2.11	(103)
O_2	2.11	(103)
CH_4	2.17	(104)
C_2H_6	2.27	(104)
C_3H_8	2.29	(104)
Average: 2.24 ± 0.09 (std. dev.)		

and carbon dioxide. (For clarity, only a representative sample of the data for a given system is plotted.) According to the mode-mode-coupling theory, all the data for Γ^* should be described by the same function of $q\xi$, which is given by Eq. (30) and is shown as the solid curve in Fig. 10. The pure fluid data have been corrected for background contributions, but for the binary-mixture data no background corrections have been made. That is, we assume that the background concentration conductivity is negligible compared to the critical part of the concentration conductivity, and we also assume that the susceptibility background is negligible for the mixtures (thus $X = X^C$).

For SF_6, since there have been no direct measurements of the density dependence of the viscosity, we have estimated the background viscosity at the critical point using the corresponding states relation $\eta_s^B(\rho_c, T_c)/\eta_s(0, T_c) = 2.24 \pm 0.09$, which we have found to hold for several other fluids: xenon,[60,97,98] CO_2,[99,100] argon,[102] krypton,[97,98] nitrogen,[103] oxygen,[103] ethane,[104] methane,[104] and propane.[104] The value of the viscosity ratio for each of these fluids is indicated in Table VI. Combining the corresponding states relation with dilute-gas viscosity data for SF_6,[105] we find $\eta_s^B(\rho_c, T) = 374 + 131\epsilon\ \mu P$. Since there have been no measurements of the critical part of the viscosity reported for SF_6, we can only make an estimate of η_s^C for SF_6 based on the measurements for other fluids. As will be shown in Sec. V, $\eta_s^C/\bar{\eta}_s$ is nearly the same for all those systems for which extensive viscosity measurements have been made. The result for this ratio [given in Table III G (a)] was used to calculate η_s^C for SF_6. Since η_s^C is a small fraction of the total viscosity in the region of interest, the uncertainty in Γ^* from this estimation procedure should be small.

The other parameters used in calculating the theoretical linewidth and the correlation length for SF_6 were taken from Refs. 10 and 35. As can be seen in Fig. 10, the SF_6 data agree quite well with the theoretical curve except for $q\xi \lesssim 0.05$, where the deviation from theory is probably due to the cell-wall-scattering problem.

The 2,6 lutidine-water mixture was studied extensively by Gulari *et al.*,[57] who measured linewidths, intensities, and viscosities. Over most of the range of $q\xi$ studied these data fall about 20% below the theoretical curve; however, as can be seen in Fig. 10, the scatter in these data is quite large.

In contrast with the 2,6 lutidine-water system, the mixtures 3 methylpentane-nitroethane[23,24] and isobutyric acid-water[61] show good agreement with the theory over the entire range of Fig. 10 except for a small, systematic departure near $q\xi = 1$.

For the mixture aniline-cyclohexane Bergé, Calmettes, Laj, and Volochine[18,19] have obtained extensive linewidth data; Calmettes, Lague, and Laj[106] have determined correlation lengths from intensity measurements; and Arcovito *et al.*[107] and Yang and Meeks[59] have measured the shear viscosity. As can be seen in Fig. 10, the aniline-cyclohexane results for Γ^* are in good agreement with the theory.

In spite of the considerable scatter in the data for Γ^* in Fig. 10, it is clear that the data for

TABLE VII. Parameters for the shear viscosity for pure fluids at the critical density and binary mixtures at the critical concentration. First the linewidth were fit to Eq. (20a) to determine $\bar{\eta}_s$; the uncertainty shown is one standard deviation. Then the data for the macroscopic shear viscosity were fit to $\eta_s^C/\bar{\eta}_s = (8/15\pi^2)\ln(q_D\xi)$ to determine q_D, which is a free parameter in the theory. In this analysis we used only those viscosity data sufficiently far from T_c ($\epsilon \gtrsim 5\times10^{-5}$) such that the density-gradient problem was not serious, and sufficiently close to T_c ($\epsilon \lesssim 2\times10^{-3}$) so that the results for η_s^C are not seriously affected by the uncertainty in the background viscosity η_s^B. References for the linewidth and shear-viscosity data used in this analysis are given in Secs. IV C and V A.

System	ξ(Å) (Ref.)	$\bar{\eta}_s$ (cP)	$\bar{\eta}_s/\eta_s^B$	$\ln(q_D\xi_0)$
Xenon	$2.00\epsilon^{-0.63}$ [8, 9]	0.0542 ± 0.0040	1.03	−2.87
CO_2	$1.50\epsilon^{-0.633}$ [81]	0.0377 ± 0.0029	1.15	−2.8 [a]
SF_6	$1.50\epsilon^{-0.67}$ [114]	0.0490 ± 0.0077	1.31	−2.8 [a]
3 methylpentane-nitroethane	$2.56\epsilon^{-0.616}$ [23, 24]	0.520 ± 0.030	1.30	−1.53
2,6 lutidine-water	$2.00\epsilon^{-0.61}$ [57]	3.65 ± 0.72	0.99	−3.14
Isobutyric acid-water	$3.62\epsilon^{-0.618}$ [61]	2.96 ± 0.72	1.28	−2.46
Aniline-cyclohexane	$2.20\epsilon^{-0.63}$ [106]	1.50 ± 0.90	1.17	−1.97

[a] Assumed.

the seven different fluid systems exhibit quite similar behavior on this "universal" plot. The systematic departure of the xenon, CO_2, and SF_6 data from the theory at small $q\xi$ could be due to failure of the mode-mode-coupling theory, incorrect background subtraction, or errors in the linewidth measurements; however, as we have mentioned, it is likely that the cell-wall-scattering problem is responsible for this departure from the theory.

On the whole, the measured values of Γ^* agree within the experimental uncertainty with the mode-mode-coupling-theory prediction that the data for Γ^* for any system for any thermodynamic path should all fall in a single universal curve which is given by Eq. (30). Note that Fig. 10 includes data not only for seven different systems, but also data for three different thermodynamic paths for xenon and carbon dioxide (the critical isochore and the two sides of the coexistence curve). Although we have included the vertex and correlation-function modifications to the theory, the data are not yet sufficiently accurate to determine whether or not these refinements of the theory are important.

V. COMPARISON OF EXPERIMENTS WITH DECOUPLED-MODE THEORY

We first examine the validity of the theoretical expression for the macroscopic shear viscosity, Eq. (20b). In this analysis $\bar{\eta}_s$ is determined by fitting the linewidth data to Eq. (20a), and then the viscosity data are fit to Eq. (20b), yielding the Debye cutoff parameter q_D. Then in Sec. V B we compare the results of linewidth measurements with the Perl and Ferrell refined decoupled-mode expression for the decay rate, Eq. (21), evaluated using the parameters $\bar{\eta}_s$ and q_D obtained in Sec. V A.

A. Viscosity

We have determined the constant $\bar{\eta}_s$ for different fluids from a least-squares fit of the linewidth data to Eq. (20a), and the results, including the standard deviation in $\bar{\eta}_s$, are given in Table VII. Equation (20a) was found to be a reasonable representation of the linewidth data, as Fig. 11 illustrates for CO_2 and Fig. 2 of Ref. 45(b) illustrates for 3 methylpentane-nitroethane.

The experimental results for the ratio $\eta_s^C/\bar{\eta}_s$, where η_s^C is the critical part of the macroscopic viscosity, are shown in Fig. 12 for six fluids. The points plotted in Fig. 12 are, except for CO_2, values calculated from the reported best-fit expressions to the viscosity data. We least-squares fit the data for $\eta_s^C/\bar{\eta}_s$ to Eq. (20b), which can be rewritten

$$\eta_s^C/\bar{\eta}_s = (8/15\pi^2)(\ln q_D \xi_0 - \nu \ln\epsilon), \tag{42}$$

where q_D is taken as a free parameter, and ξ_0, ν, and $\bar{\eta}_s$ are known from other measurements. The results of this analysis are given in Table VII, which also includes the ratio $\bar{\eta}_s/\eta_s^B$ that enters the expression for η_s^{eff} [Eq. (21b)]. In the semi-log plot in Fig. 12 the adjustable parameter q_D determines the vertical position of the line, while the slope of the line is given by $-\nu(8/15\pi^2) \simeq -0.034$. As can be seen in Fig. 12, all the data for η_s^C are described reasonably well by the predicted logarithmic temperature dependence.

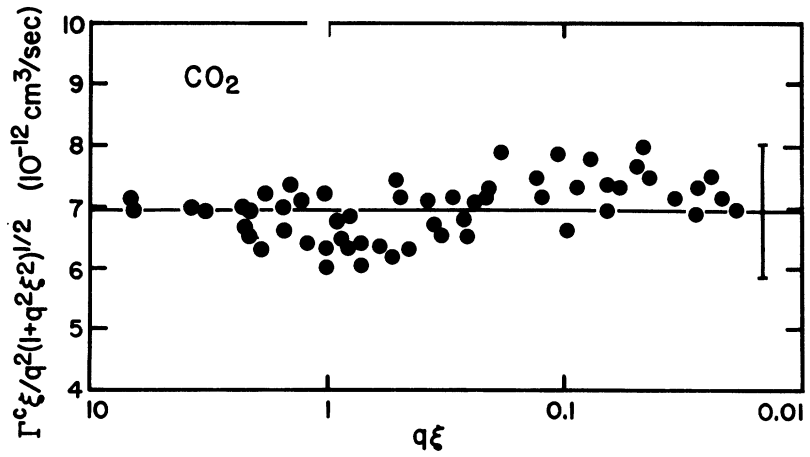

FIG. 11. The quantity $\Gamma^C/q^2(q^2+\xi^{-2})^{1/2}$ is shown as a function of $q\xi$ for CO_2. (Data for which $q\xi \lesssim 0.035$ have been omitted due to the cell-wall-scattering problem.) The mean value of the data gives $\bar{\eta}_s = 377 \pm 29$ μP, where the uncertainty is one standard deviation. The horizontal line represents the mean value of the data, and the error bar indicates ± two standard deviations from the mean value.

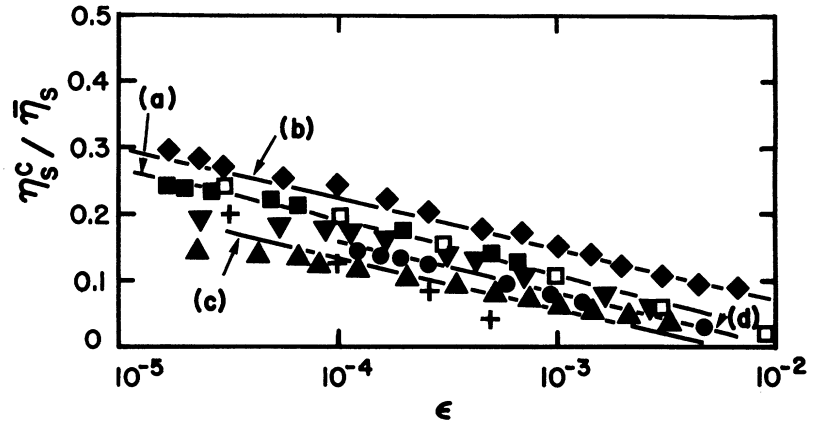

FIG. 12. Experimental results for the ratio $\eta_s^C/\bar{\eta}_s$, where η_s^C is the critical part of the measured macroscopic viscosity, and $\bar{\eta}$ is a parameter (given in Table VII) obtained by fitting linewidth data to Eq. (20a). The critical part of the viscosity was calculated for the different fluids using the best-fit equations from the original papers: □, aniline-cyclohexane data of Arcovito *et al.* (Ref. 107); ■, aniline-cyclohexane data of Yang and Meeks (Ref. 59); ◆, 3 methylpentane-nitroethane (Ref. 58); ▼, isobutyric acid-water (Ref. 108); ▲, 2,6 lutidine-water (Ref. 57); ●, xenon (Refs. 60, 97, and 98); +, extrapolated CO_2 data (Refs. 60, 99, and 100). The straight lines show the results of fitting the viscosity data to $\eta_s^C/\bar{\eta}_s = (8/15\pi^2)\ [\ln q_D\xi_0 - \nu \ln\epsilon]$, with q_D taken as an adjustable parameter and $\bar{\eta}_s$ and ξ given by the values in Table VII. For clarity, the curves are shown only for four fluids: (a) aniline-cyclohexane, (b) 3 methylpentane-nitroethane, (c) 2,6 lutidine-water, and (d) xenon.

For pure fluids there is an established systematic procedure for calculating the background viscosity using data obtained outside the critical region, as we have discussed in Sec. II A, but the same approach cannot be applied to most binary mixtures because extensive data as a function of concentration and temperature do not exist. Therefore, the reported values for the background viscosity for mixtures were deduced either by fitting viscosity data obtained in the critical region to an expression which includes both the background and critical parts or by extrapolating into the critical region data obtained far from the critical point. As several authors have discussed, the same viscosity data can appear to exhibit a cusp or a weak divergence at the critical point, depending on the particular procedure used to deduce η_s^B (see Sec. II F and the recent review by Sengers[109]).[57,58]

Included in Fig. 12 are a few points for CO_2 obtained in independent experiments by Strumpf *et al.*[60] and Kestin *et al.*[99] These data, which were obtained by extrapolation to the critical isochore of data obtained off the critical isochore, agree fairly well with the values of $\eta_s^C/\bar{\eta}_s$ measured for other fluids; therefore, in our analysis of the CO_2 linewidth data we have used an expression, shown by curve (c) in Fig. 12 and given in Table III G(a), which describes reasonably well the viscosity ratio for different fluids.

B. Decay Rate

The decoupled-mode-theory expression for the decay rate is

$$\Gamma^C = C(q\xi)\left(\frac{K_0(q\xi)}{(q\xi)^3}\right)\left(\frac{k_B T}{6\pi\eta_s^{\text{eff}}}\right), \tag{43}$$

where we have included the correlation-function correction term $C(q\xi)$, which increases monotonically from $C(0)=1.014$ to $C(\infty)=1.056$ (see Sec. II E). We could compare Eq. (43) directly with the experimental values for Γ^C; however, since Γ^C is quite different for different fluids, the comparison between theory and experiment and the comparison between the decoupled-mode theory and the mode-mode-coupling theory is facilitated by again considering the scaled linewidth

$$\Gamma^* \equiv (6\pi\eta_s\Gamma^C/k_B T q^3),$$

which in the decoupled-mode theory is given by

$$\Gamma^* = C(q\xi)\left(\frac{K_0(q\xi)}{(q\xi)^3}\right)\left(\frac{1+(\bar{\eta}_s A/\eta_s^B)\ln(q_D\xi)}{1+(\bar{\eta}_s A/\eta_s^B)[\ln(q_D\xi)-\frac{1}{2}\ln(1+q^2\xi^2)+\tau(q\xi)]}\right), \tag{44}$$

where $A = 8/15\pi^2$. Here the scaled linewidth is not a universal function of the single variable $q\xi$, as it is in the mode-mode-coupling theory. However, if we rewrite Eq. (44) as

$$\Gamma^* = C(q\xi)\left(\frac{K_0(q\xi)}{(q\xi)^3}\right)\left\{1+\left(\frac{\bar{\eta}_s A}{\eta_s^B}\right)\left[\tfrac{1}{2}\ln(1+q^2\xi^2)-\tau(q\xi)\right]\right.$$
$$\left.+-\left(\frac{\bar{\eta}_s A}{\eta_s^B}\right)^2\left[\ln(q_D\xi)-\tfrac{1}{2}\ln(1+q^2\xi^2)+\tau(q\xi)\right]\left[\tfrac{1}{2}\ln(1+q^2\xi^2)-\tau(q\xi)\right]+\ldots\right\}, \quad (45)$$

then it is clear that Γ^* is a function only of $q\xi$ if the second- and higher-order terms in A can be neglected. In the hydrodynamic region the contribution of the higher-order terms is less than 0.5% for $\epsilon < 3\times10^{-2}$, while in the nonhydrodynamic region the contribution of the higher-order terms is larger, but still typically less than 3%, for the data which we analyze in this paper. The decoupled-mode expression [Eq. (45)] for Γ^* with the second and higher terms in A neglected is compared with the mode-mode-coupling theory [Eq. (30)] in Fig. 13. The upper and lower curves shown for the decoupled-mode theory correspond, respectively, to the values of $\bar{\eta}_s/\eta_s^B$ obtained for 3 methylpentane-nitroethane ($\bar{\eta}_s/\eta_s^B = 1.30$) and 2,6 lutidine-water ($\bar{\eta}_s/\eta_s^B = 0.99$); for the other fluids considered here the ratio $\bar{\eta}_s/\eta_s^B$ falls between 1.30 and 0.99.

In the hydrodynamic region the mode-mode-coupling theory (with vertex corrections included) yields

$$\Gamma^* = 1.053/q\xi, \quad (46)$$

while the decoupled-mode theory (including higher-order terms in A) yields

$$\Gamma^* = (1.050 \pm 0.003)/q\xi, \quad (47)$$

where the ±0.003 in Eq. (47) is due to the small, $q\xi$-dependent contribution of the higher-order terms. Thus the two theories are in excellent agreement in the hydrodynamic region. However, as noted in Sec. IID, the decoupling approximation is equivalent to the neglect of vertex corrections; if the comparison of the decoupled-mode theory with the mode-mode-coupling theory is made with the vertex corrections omitted from the latter theory, then the mode-mode-coupling values for Γ^* are 2.7% instead of 0.3% higher than the decoupled-mode values for Γ^* in the hydrodynamic region.

The difference between the mode-mode-coupling and decoupled-mode theories is much larger in the extreme nonhydrodynamic region; e.g., at $q\xi = 10$ the difference between the two theories (with the higher-order terms in the decoupled-mode theory neglected) is 8.3% for $\bar{\eta}_s/\eta_s^B = 1.30$ and 12.5% for $\bar{\eta}_s/\eta_s^B = 0.99$. In the extreme nonhydrodynamic region the omission of vertex corrections would lower the mode-mode-coupling-theory values for Γ^* by only 0.4%; thus the vertex corrections are far too small to explain the difference between the two theories in this region.

In Fig. 14 we compare the data for Γ^* for four fluids with the decoupled-mode and mode-mode-coupling theories. In Fig. 14, only the region for which $q\xi > 0.1$ is shown, since the two theories are essentially in agreement in the hydrodynamic region. Although the amount of data in the nonhydrodynamic region is limited, the available data can be seen (Fig. 14) to be in somewhat better agreement with the decoupled-mode theory than with the mode-mode-coupling theory. Additional data in the nonhydrodynamic region are clearly needed; however, this is a region in which definitive experiments are quite difficult, because of the density-gradient, concentration-gradient, and temperature-control problems.

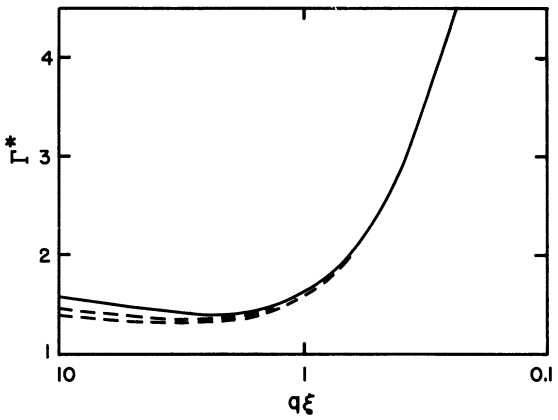

FIG. 13. The theoretical predictions for the scaled linewidth, $\Gamma^* = 6\pi\eta_s\Gamma^C/k_BTq^3$, in the mode-mode-coupling and the decoupled-mode theories. The mode-mode-coupling calculation of Lo and Kawasaki yields a single, universal curve for Γ^*, which is shown by the upper curve (Refs. 43 and 44). Perl and Ferrell found that the decoupled-mode approach leads to a result for Γ^* that is slightly different for different fluids, depending on the ratio $\bar{\eta}_s/\eta_s$ (see Table VII) (Refs. 45 and 46). However, for the fluids we consider in this paper the ratio $\bar{\eta}_s/\eta_s^B$ falls within the range between 1.30 and 0.99, which are the values used in drawing the upper and lower dashed curves, respectively. The curves for the decoupled-mode theory represent the theory to lowest order in $A = 8/15\pi^2$; if higher-order terms in A were included, the theoretical values for Γ^* would be changed typically by 3% or less, but would depend not only on $q\xi$ but also on q_D [see Eq. (44)]. The curves for both the mode-mode and decoupled-mode theories include the correlation-function modification $C(q\xi)$ (see Sec. IIE).

VI. CONCLUSIONS

We have shown that within the experimental uncertainty the data for the dimensionless quantity $\Gamma^* = 6\pi\eta_s\Gamma^C/k_BTq^3$, the "scaled linewidth," are all described by the same universal function of the variable $q\xi$, independent of the particular thermodynamic path or fluid system (see Fig. 10). We have also shown that the mode-mode-coupling-theory and decoupled-mode-theory predictions for the scaled linewidth are essentially the same, except in the extreme nonhydrodynamic region ($q\xi >> 1$), where the decoupled-mode values for Γ^* are ~10% smaller than those predicted by the mode-mode-coupling theory. Furthermore, the experimental results for Γ^* agree with the theoretical predictions within the combined uncertainties (~10%) of theory and experiment.[110] This remarkable result is illustrated in Figs. 10 and 14; it should be emphasized that this comparison between theory and experiment involves no adjustable parameters, since the theoretical expressions were evaluated using independently determined shear-viscosity and correlation-length data. Although the theoretical predictions of the mode-mode-coupling and decoupled-mode theories differ by ~10% in the extreme nonhydrodynamic region, the data in this region are sparse and have too much scatter to distinguish clearly between the two theories.

The accuracy of ~10% in the present comparison of the theory with the experimental data for different systems could be improved to approach ~1% if currently available techniques for measuring and controlling temperature and for measuring Γ, ξ, and η_s were fully exploited. We will now summarize some of the principal experimental and theoretical difficulties which arise in attempting to achieve an accuracy of 1% in an absolute comparison of the theoretical and experimental values of the decay rate.

A. Experimental Problems

With the recently developed digital autocorrelation technique, it is now possible to perform individual measurements of the decay rate with a statistical uncertainty of less than 1%[111]; however, the fluctuations in the individual values of Γ measured for a fluid at a particular temperature and density (or concentration) in all of the reported experiments is much larger, typically ~ ±6% (see the graphs of Γ in the original papers for any of the fluids that have been investigated). These

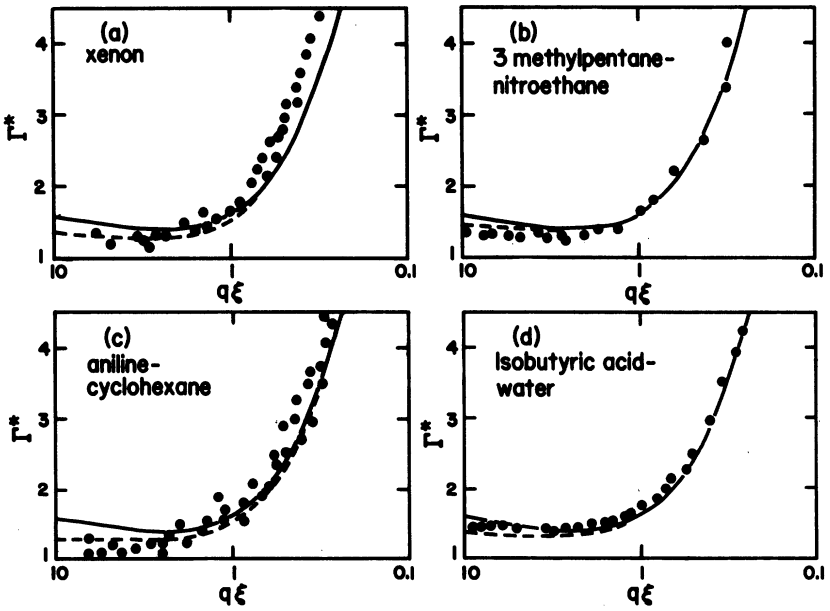

FIG. 14. A comparison of the experimental results for Γ^* with the decoupled-mode and mode-mode-coupling theories: (a) xenon, (b) 3 methylpentane-nitroethane, (c) aniline-cyclohexane, (c) isobutyric acid-water. For each fluid the solid curve represents the mode-mode-coupling theory (Refs. 40, 44, and 47) with viscosity, vertex, and correlation-function modifications included, and the dashed curve represents the decoupled-mode theory (Refs. 41, 45, and 46) with the viscosity and correlation-function modifications included. In the decoupled-mode theory there is a small variation in Γ^* at a given value of $q\xi$ due to the higher-order terms in Eq. (45); however, this variation is typically less than 2% for the range of q and ξ investigated in the experiments considered here, which is too small to show on the scale of these graphs.

fluctuations are due in part to insufficient long-term temperature stability and equilibration. In recent measurements on xenon in our laboratory Lim[10] has maintained the sample temperature within 0.5 mK for periods of days, and the temperature gradients in the thermostat oil bath have been reduced to less than 0.5 mK by vigorous stirring; with these precautions the individual measurements of the linewidth performed with a digital autocorrelator over periods of months for a particular temperature and beam height in the sample cell reproduce to within 1%.

In the reported investigations of the linewidth for binary mixtures near the critical point, insufficient attention has been paid to the problem of the gravitationally produced density and concentration gradients. As Mistura has pointed out, the density gradient in a binary mixture is proportional to the thermodynamic derivative $(\partial\rho/\partial P)_{T,\Delta}$, which corresponds to the isothermal compressibility of a pure substance and is strongly divergent at the critical point.[112,113] Moreover, the concentration gradient near the critical point is proportional to the density gradient, although the proportionality constant may be small for some mixtures (the coefficient of proportionality is zero if the critical point happens to fall on the azeotropic line.[112] Our linewidth measurements in CO_2, xenon, and SF_6 have all been performed as a function of beam height in the sample cell, and we have found that the dependence of the linewidth on height is large near T_c (see Fig. 2),[2-6,8,10] and unless the thermostat temperature is extremely stable and uniform, the height corresponding to the minimum Γ varies with time. Although the dependence of Γ on height may well be small even very near T_c for some mixtures, in general it will not be negligible; hence future linewidth measurements for mixtures near the critical point should explore the height dependence of Γ.

Shear-viscosity and correlation-length data are needed in order to compare the results of linewidth measurements with the theories. The most extensive measurements of the correlation length for a fluid near a critical point have been performed for CO_2; for this fluid Lunacek and Cannell obtained accurate values for ξ by using a differential technique to determine the angular dependence of the scattering intensity for temperatures ranging over three orders of magnitude in ΔT.[81,114] More measurements of this type are clearly needed for other systems.

Extensive measurements of the shear viscosity near the critical point have been reported for many binary mixtures and for xenon, CO_2, and ethane (see the review by Sengers[109]). Most of these measurements were performed with capillary-flow viscometers, which actually determine the kinematic viscosity η_s/ρ. In the capillary viscometers there is a pressure gradient across a tube several centimeters long; hence the accuracy of this method is seriously limited very near T_c by the density and composition gradients. In an alternative technique, which has the advantage that it does not produce a macroscopic pressure difference in the sample, the viscosity is determined from measurements of the damping constant of a small torsionally oscillating cylinder or disc; however, the interpretation of a characteristic damping time in terms of a viscosity is not entirely straightforward, especially near T_c.

A very interesting different approach to the study of the viscosity of fluids near the critical point was used recently by Lyons, Mockler, and O'Sullivan,[63] who used light-beating spectroscopy to determine the diffusion coefficient D of Brownian particles in the mixture nitroethane-iso-octane near the critical point. Measurements of D for the Teflon microspheres (diam $d = 0.31$ μm) in their mixture yielded a value for the effective viscosity through the Stokes-Einstein relation, $D = k_B T/3\pi\eta_s d$. There are no macroscopic disturbances of the sample for this technique, and the region probed is only ~0.1 mm high (the diameter of the focused laser beam). Thus this technique can potentially yield information on the viscosity very near T_c, a region in which accurate measurements are needed if the nonhydrodynamic ($q\xi \gtrsim 1$) behavior of the decay rate is to be compared with the theoretical predictions. The promise of this technique hinges on a better understanding of the relation between D and η_s, especially very near T_c, where $\xi \sim d$.

B. Theoretical Problems

The effect of the large, relatively slow, long-wavelength order-parameter fluctuations on dynamical behavior near the critical point was considered in Ferrell's decoupled-mode calculation and in Kawasaki's mode-mode-coupling calculation, but in both approaches to the calculation of the critical behavior of transport coefficients, the effect of the high-frequency fluctuations which give rise to the "background part" of the transport coefficients, was neglected.[115,116] Since the theories neglect the background contributions to the decay rate, any comparison of theory and experiment must include a well-reasoned systematic method for extracting the critical part of the decay rate Γ^C from the measured values Γ. For the single-component fluids we have used a modified Sengers-Keyes ansatz in making the background correction, a procedure which seems to be sys-

tematic and self-consistent (see Sec. IIA). On the other hand, we have not been able to make any quantitative estimate of the background contributions for the binary mixtures, so that the rather good agreement between theory and experiment illustrated for the binary mixtures in Fig. 10 must be regarded as perhaps in part fortuitous, especially for small $q\xi$, where the background contribution may well be significant.

The mode-mode-coupling expression [Eq. (24)] that we have used for the decay rate cannot represent the full mode-mode-coupling theory since, in addition to the absence of background corrections, intermediate states with three or more modes (representing higher-order nonlinearities) were not included in the derivation.[40,43,47] Also, only the four lowest-order vertex-correction terms were considered in the derivation of Eq. (24), and these vertex corrections were evaluated only in the limits $q\xi \ll 1$ and $q\xi \gg 1$; however, the vertex corrections were found to be only 2.44% or less for the cases considered.

The refined decoupled-mode expression of Perl and Ferrell was derived starting with an ansatz for Γ^C, Eq. (20a), which was found to give a good fit to the experimental data.[45,46] This ansatz involves an adjustable parameter $\bar{\eta}_s$ (to be determined by fitting the linewidth data), which then appears in the final expression for the decay rate. Another adjustable parameter in the Perl-Ferrell theory is q_D, the "Debye cutoff," which is to be determined by fitting the critical part of the viscosity of Eq. (20b). Thus the decoupled-mode-theory predictions for Γ^*, unlike those of the mode-mode-coupling theory, are different for different fluids, depending on the values of $\bar{\eta}_s$ and q_D. However, the decoupled-mode predictions for Γ^* for different fluids differ by only a few tenths of a percent in the hydrodynamic region and by not more than a few percent in the nonhydrodynamic region. Another difference between the mode-mode-coupling and the decoupled-mode theories is that while the mode-mode-coupling value of Γ^* depends only on the *product* of q and ξ, in the decoupled-mode theory the value of Γ^* depends not only on $q\xi$ but also [due to the higher-order terms in Eq. (45)] on the individual values of q and ξ. Yet another difference between the mode-mode-coupling and decoupled-mode theories is that the decoupling approximation necessarily excludes vertex corrections, as was discussed in Sec. IID.

The effect of departures from Ornstein-Zernike correlations was discussed in Sec. IIE, where the correlations were assumed to be described by the function $\hat{G}_{\mathrm{FB}}$ obtained by Fisher and Burford for the Ising model. However, the amount of experimental evidence on the proper functional form for the correlation function for real fluids and magnets is quite limited, and, as has been shown in Ref. 48, the correction of Γ^C calculated using $\hat{G}_{\mathrm{FB}}$ is qualitatively different from the correction calculated using other forms for $\hat{G}$ that have sometimes been used to describe departures from Ornstein-Zernike behavior in scattering experiments. With the correlations described by $\hat{G}_{\mathrm{FB}}$ the correction to Γ^C increases with increasing $q\xi$, while for the other correlation functions considered in Ref. 48 the correction decreases with increasing $q\xi$. The magnitude of the correction is typically several percent, depending, of course, not only on the form of G but also on the value of the exponent η, which is not well established.

C. Summary

We have compared the results of Rayleigh-linewidth measurements on pure fluids and binary mixtures near the critical point with the specific predictions of the mode-mode-coupling and decoupled-mode theories. These theories constitute more complete theories of dynamical behavior than the dynamic-scaling theory, in which the function $f(q, \xi^{-1})$ in Eq. (12) is *any* homogeneous function of q and ξ^{-1} of degree z; nevertheless it should be noted that the data in Fig. 10 are consistent with the dynamic-scaling prediction.

The agreement of the linewidth data with the theoretical predictions is remarkably good, considering the experimental and theoretical difficulties enumerated above in Secs. VIA and VIB. The predictions of the mode-mode and decoupled-mode theories do not differ significantly, except in the extreme nonhydrodynamic region, where the difference is ~10%; there, the scaled linewidths appear to be described somewhat better by the decoupled-mode theory than the mode-mode-coupling theory, as Fig. 14 illustrates, but this result is at most suggestive rather than conclusive, since the available data in the extreme nonhydrodynamic region are sparse and exhibit considerable scatter.

More-accurate linewidth, viscosity, and correlation-length data are required, especially near T_c, if the theories are to be tested further. If the theories with all significant corrections can be established from measurements of the linewidth, viscosity, and the sound velocity and attenuation, the linewidth measurements should yield information on the proper form of the correlation function for fluids near the critical point.[48]

ACKNOWLEDGMENTS

We are happy to acknowledge helpful discussions with Professor K. Kawasaki, Professor R. B.

Griffiths, Professor R. A. Ferrell, Dr. P. C. Hohenberg, and Dr. R. Perl. We also thank Dr. Perl for reports of his work prior to publication and for a critical reading of this manuscript. We thank Dr. H. F. Strumpf, Dr. A. F. Collings, and Professor C. J. Pings for tables of their xenon and CO_2 viscosity data; Dr. Erdogan Gülari for tables of linewidth data for 2, 6 lutidine-water; Dr. B. Volochine and Dr. P. Bergé for tables of linewidth data for aniline-cyclohexane; and Professor J. V. Sengers for reports of his work prior to publication. We are especially grateful to Dr. T. K. Lim, who took much of the xenon linewidth data and assisted in the analysis, and to Professor H. Z. Cummins for his encouragement and support and for many stimulating discussions throughout the course of this research. Finally, one of us (D.L.H.) thanks Professor R. Kobayashi and the Petroleum Research Fund (administered by the American Chemistry Society) for support during the preparation of this paper.

---

*Research supported by the National Science Foundation.

†Present address: City College, Department of Physics, Convent Avenue and 138th Sts., New York, N.Y. 10031.

[1]L. Van Hove, Phys. Rev. 95, 1374 (1954); see also L. D. Landau and I. M. Khalatnikov, Dokl. Akad. Nauk SSSR 90, 469 (1954).

[2]H. L. Swinney and H. Z. Cummins, Phys. Rev. 171, 152 (1968).

[3]H. L. Swinney, Ph.D. thesis (Johns Hopkins University, 1968) (unpublished).

[4]D. L. Henry, H. L. Swinney, and H. Z. Cummins, Phys. Rev. Lett. 25, 1170 (1970).

[5]D. L. Henry, Ph.D. thesis (Johns Hopkins University, 1970) (unpublished).

[6]H. L. Swinney, D. L. Henry, and H. Z. Cummins, J. Phys. (Paris) Suppl. 33, C1-81 (1972).

[7]B. S. Maccabee and J. A. White, Phys. Rev. Lett. 27, 495 (1971).

[8]T. K. Lim, H. L. Swinney, I. W. Smith, and G. B. Benedek, Opt. Commun. 7, 18 (1973).

[9]I. W. Smith, Ph.D. thesis (MIT, 1972) (unpublished); see also Ref. 101.

[10]T. K. Lim, Ph.D. thesis (Johns Hopkins University, 1973) (unpublished).

[11]G. B. Benedek, in *Polarization, Matière et Rayonnement, Livre de Jubilè en l'honneur du Professeur A. Kastler,* edited by The French Physical Society (Presses Universitaires de France, Paris, France, 1969), p. 49.

[12]H. Z. Cummins and H. L. Swinney, in *Progress in Optics,* edited by E. Wolf (North-Holland, Amsterdam, 1970), Vol. VIII, p. 133.

[13]B. Chu, Ann. Rev. Phys. Chem. 21, 145 (1970).

[14]H. Z. Cummins, in *Critical Phenomena, International School of Physics "Enrico Fermi," LI Course, 1970,* edited by M. S. Green (Academic, New York, 1971), p. 380.

[15]S. S. Alpert, Y. Yeh, and E. Lipworth, Phys. Rev. Lett. 14, 486 (1965).

[16]N. C. Ford, Jr., and G. B. Benedek, Phys. Rev. Lett. 15, 649 (1965).

[17]R. D. Mountain, Rev. Mod. Phys. 38, 205 (1966).

[18]P. Berge, P. Calmettes, C. Laj, and B. Volochine, Phys. Rev. Lett. 23, 693 (1969).

[19]P. Berge, P. Calmettes, C. Laj, M. Tournarie, and B. Volochine, Phys. Rev. Lett. 24, 1223 (1970).

[20]B. Chu, F. J. Schoenes, and W. P. Kao, J. Am. Chem. Soc. 90, 3042 (1968); B. Chu, J. Chem. Phys. 47, 3816 (1967).

[21]S. H. Chen and N. Polonsky-Ostrowsky, Opt. Comm. 1, 64 (1969).

[22]P. N. Pusey and W. I. Goldburg, Phys. Rev. Lett. 23, 67 (1969).

[23]R. F. Chang, P. H. Keyes, J. V. Sengers, and C. O. Alley, Phys. Rev. Lett. 27, 1706 (1971).

[24]R. F. Chang, P. H. Keyes, J. V. Sengers, and C. O. Alley, Ber. Bunsenges. Phys. Chem. 76, 260 (1972).

[25]G. B. Benedek, in *Statistical Physics, Phase Transitions, and Superfluidity,* edited by M. Chretien *et al.* (Gordon and Breach, New York, 1968), Vol. 2, p. 1; and in *Proceedings of the Fourteenth International Solvey Conference in Chemistry,* edited by R. Defay (Wiley, London, 1970).

[26]C. S. Bak and W. I. Goldburg, Phys. Rev. Lett. 23, 1218 (1969).

[27]C. S. Bak, W. I. Goldburg, and P. N. Pusey, Phys. Rev. Lett. 25, 1420 (1970); W. I. Goldburg and P. N. Pusey, J. Phys. (Paris) Suppl. 33, C1-105 (1972).

[28]J. V. Sengers, in Ref. 14, p. 445.

[29]M. E. Fisher, Rept. Progr. Phys. 30, 615 (1967).

[30]J. V. Sengers and P. H. Keyes, Phys. Rev. Lett. 26, 70 (1971).

[31]G. B. Benedek, J. B. Lastovka, M. Giglio, and D. Cannell, in *Critical Phenomena in Alloys, Magnets, and Superconductors,* edited by R. E. Mills, E. Ascher, and R. I. Jaffe (McGraw-Hill, New York, 1971), p. 503.

[32]N. Throdorakopoulos, Ph.D. thesis (Brown University, 1972) (unpublished).

[33]P. Braun, D. Hammer, W. Tscharnuter, and P. Weinzierl, Phys. Lett. A 32, 390 (1970).

[34]R. Mohr and K. H. Langley, J. de Phys. (Paris) Suppl. 33, C1-81 (1972).

[35]T. K. Lim, H. L. Swinney, K. H. Langley, and T. A. Kachnowski, Phys. Rev. Lett. 27, 1776 (1971).

[36]G. T. Feke, G. A. Hawkins, J. B. Lastovka, and G. B. Benedek, Phys. Rev. Lett. 27, 1780 (1971); see also G. T. Feke, J. B. Lastovka, G. B. Benedek, K. H. Langley, and P. B. Elterman, Opt. Commun. 7, 13 (1973).

[37]M. Fixman, J. Chem. Phys. 36, 310 (1962); Adv. Chem. Phys. 6, 175 (1964); see also J. Chem. Phys. 36, 1363 (1960).

[38]K. Kawasaki, Phys. Rev. 150, 291 (1966). For a discussion of the Kubo formulas for the different transport coefficients see, for example, R. Zwanzig, Ann. Rev. Phys. Chem. 16, 67 (1965).

[39]L. P. Kadanoff and J. Swift, Phys. Rev. 166, 89 (1968); L. P. Kadanoff, J. Phys. Soc. Japan Suppl. 26, 122 (1969).
[40]K. Kawasaki, Phys. Lett. A 30, 325 (1969); Ann. Phys. (New York) 61, 1 (1970); Phys. Rev. A 1, 1750 (1970).
[41]R. A. Ferrell, Phys. Rev. Lett. 24, 1169 (1970). The comparison between the mode-mode-coupling and the decoupled-mode theories is discussed by R. A. Ferrell [in *Dynamical Aspects of Critical Phenomena*, edited by J. I. Budnick and M. P. Kawatra (Gordon and Breach, New York, 1972), p. 1 (see, in particular, Fig. 1)].
[42]B. Chu, D. Thiel, W. Tscharnuter, and D. V. Fenby, J. Phys. (Paris) 33, C1-111 (1972).
[43]K. Kawasaki and S. M. Lo, Phys. Rev. Lett. 29, 48 (1972). The critical behavior of the shear viscosity in the hydrodynamic region is also discussed by K. Kawasaki in Ref. 14, p. 342; and in *Critical Phenomena in Alloys, Magnets, and Superconductors*, edited by R. E. Mills, E. Ascher, and R. I. Jaffe (McGraw-Hill, New York, 1971), p. 489. These last two references give $(16/15\pi^2)$ for the numerical coefficient in the expression for the critical part of the macroscopic shear viscosity, but this number was subsequently revised to $(8/15\pi^2)$, as given in our Eq. (20b) [see Ref. 15 of R. Perl and R. A. Ferrell, Phys. Rev. A 6, 2358 (1972)].
[44]S. M. Lo and K. Kawasaki, Phys. Rev. A 8, 2176 (1973).
[45](a) R. Perl and R. A. Ferrell, Phys. Rev. Lett. 29, 51 (1972); (b) Phys. Rev. A 6, 2358 (1972). These papers consider the effect of the frequency and wavenumber dependence of the viscosity on the decay rate in the extreme nonhydrodynamic limit, $q\xi \gg 1$. The more general case, with $q\xi$ arbitrary, is treated in Ref. 46.
[46]R. Perl and R. A. Ferrell (unpublished).
[47]S. M. Lo and K. Kawasaki, Phys. Rev. A 5, 421 (1972).
[48](a) H. L. Swinney and B. E. A. Saleh, Phys. Rev. A 7, 747 (1973); (b) P. deGennes, The Second International Conference on Light Scattering in Solids, Paris, 1971 (unpublished).
[49]B. Widom, J. Chem. Phys. 43, 3898 (1965).
[50]L. P. Kadanoff, Physics (N.Y.) 2, 263 (1966); L. P. Kadanoff *et al.*, Rev. Mod. Phys. 39, 395 (1967).
[51]R. A. Ferrell, N. Menyhard, H. Schmidt, F. Schwabl, and P. Szepfalusy, Phys. Rev. Lett. 18, 891 (1967); Phys. Lett. A 24, 493 (1967); Ann. Phys. (N.Y.) 47, 565 (1968).
[52]B. I. Halperin and P. C. Hohenberg, Phys. Rev. 177, 952 (1969).
[53]A. Hankey and H. E. Stanley, Phys. Rev. B 6, 3515 (1972).
[54]M. E. Fisher and R. J. Burford, Phys. Rev. 156, 583 (1967); see also D. S. Ritchie and M. E. Fisher, Phys. Rev. B 5, 2668 (1972).
[55]K. Kawasaki (private communication).
[56]B. Chu, N. Kuwahara, and D. V. Fenby, Phys. Lett. A 32, 131 (1970).
[57]E. Gulari, A. F. Collings, R. L. Schmidt, and C. J. Pings, J. Chem. Phys. 56, 6169 (1972).
[58]A. Stein, J. C. Allegra, and G. F. Allen, J. Chem. Phys. 55, 4265 (1971); A. Stein, S. J. Davidson, J. C. Allegra, and G. F. Allen, J. Chem. Phys. 56, 6164 (1972).
[59]C. C. Yang and F. R. Meeks, J. Phys. Chem. 75, 2619 (1971).
[60]H. J. Strumpf, A. F. Collings, and C. J. Pings (unpublished).
[61]B. Chu, S. P. Lee, and W. Tscharnuter, Phys. Rev. A 7, 353 (1973).
[62]J. V. Sengers, Ber. Bunsenges. Phys. Chem. 76, 234 (1972).
[63]K. B. Lyons, R. C. Mockler, and W. J. O'Sullivan, Phys. Rev. Lett. 30, 42 (1973).
[64]D. H. Garside, H. V. Molgaard, and B. L. Smith, J. Phys. B 1, 449 (1968).
[65]A. B. Cornfield and H. Y. Carr, Phys. Rev. Lett. 29, 28 (1972).
[66]E. A. Guggenheim, J. Chem. Phys. 13, 253 (1945).
[67]J. V. Sengers, J. Heat Mass Transfer 8, 1103 (1965).
[68]J. A. Chapman, P. C. Finnimore, and B. L. Smith, Phys. Rev. Lett. 21, 1306 (1968).
[69]J. M. H. Levelt Sengers, J. Straub, and M. Vicentini-Missoni, J. Chem. Phys. 54, 5034 (1971).
[70]A. Michels and J. Hamers, Physica (Utrecht) 4, 995 (1937).
[71]The autocorrelator is similar in design to that of R. Foord *et al.*, Nature (Lond.) 227, 242 (1970).
[72]The precision of the fit of a measured spectrum (or correlation function) to one or more Lorentzian terms (or one or more exponential terms) is discussed by D. E. Koppel [J. Chem. Phys. 57, 4814 (1972)].
[73]H. W. Habgood and W. G. Schneider, Can. J. Chem. 32, 98 (1954).
[74]J. M. H. Levelt Sengers and W. T. Chen, J. Chem. Phys. 56, 595 (1972).
[75]M. Vincenti-Missoni, J. M. H. Levelt Sengers, and M. S. Green, J. Res. Natl. Bur. Std. (U. S.) A 73, 563 (1969); M. Vicentini-Missoni, R. I. Joseph, M. S. Green, and J. M. H. Levelt Sengers, Phys. Rev. B 1, 2312 (1970).
[76]M. S. Green, M. J. Cooper, and J. M. H. Levelt Sengers, Phys. Rev. Lett. 26, 492 (1971).
[77]A. Michels, T. Wassenaar, G. J. Wolkers, and J. Dawson, Physica (Utrecht) 22, 17 (1956).
[78]F. Theeuwes and R. J. Bearman, J. Chem. Therm. 2, 501 (1970).
[79]M. Giglio and G. B. Benedek, Phys. Rev. Lett. 23, 1145 (1969). See also Ref. 101.
[80]I. W. Smith, M. Giglio, and G. B. Benedek, Phys. Rev. Lett. 27, 1556 (1971). See also Ref. 101.
[81]J. H. Lunacek and D. S. Cannell, Phys. Rev. Lett. 27, 841 (1971).
[82]J. A. White and B. S. Maccabee, Phys. Rev. Lett. 26, 1468 (1971).
[83]C. Edwards, J. Lipa, and M. J. Buckingham, Phys. Rev. Lett. 20, 496 (1968).
[84]H. H. Schmidt, J. Opdycke, and C. F. Gay, Phys. Rev. Lett. 19, 887 (1967).
[85]H. W. Habgood and W. G. Schneider, Can. J. Chem. 32, 164 (1954).
[86]J. A. Lipa, C. Edwards, and M. J. Buckingham, Phys. Rev. Lett. 25, 1086 (1970).
[87]G. T. Feke, K. Fritsch, and E. F. Carome, Phys. Rev. Lett. 23, 1282 (1969).
[88]P. E. Mueller, D. Eden, C. W. Garland, and R. C. Williamson, Phys. Rev. A 6, 2272 (1972).
[89]C. M. Herget, J. Chem. Phys. 8, 537 (1940).
[90]H. D. Parbrook and E. G. Richardson, Proc. Royal Soc. B 65, 437 (1952).
[91]H. Tielsch and H. Tanneberger, Z. Phys. 137, 256 (1954).
[92]V. K. Saxena and S. C. Saxena, J. Chem. Phys. 51, 3361 (1969).

[93]W. G. Kannuluik and E. H. Carman, Proc. Roy. Soc. B 65, 701 (1952).
[94]A. Michels, J. V. Sengers, and P. S. van der Gulik, Physica (Utrecht) 28, 1216 (1962).
[95]B. LeNeindre, P. Bury, R. Tufeu, P. Johannin, and B. Vodar, in *Proceedings of the Ninth Thermal Conductivity Conference*, edited by H. R. Shanks (U. S. Atomic Energy Commission, Division of Technical Information Extension, Oak Ridge, Tenn., 1970), p. 169.
[96]R. Tufeu, Ph.D. thesis (University of Paris, 1971) (unpublished); see also R. Tufeu, B. LeNeindre, and P. Bury, Compt. Rend. B 273, 113 (1971).
[97]E. G. Reynes and G. Thodos, Physica (Utrecht) 30, 1529 (1964).
[98]R. A. Dawe and E. B. Smith, J. Chem. Phys. 52, 693 (1970).
[99]J. Kestin, J. H. Whitelaw, and T. F. Zien, Physica (Utrecht) 30, 161 (1964).
[100]A. Gosh, P. Chappeler, and R. Kobayashi (unpublished); J. Kestin and J. H. Whitelaw, Physica (Utrecht) 29, 335 (1963); and A. Michels, A. Botzen, and W. Shuurman, Physica (Utrecht) 23, 95 (1957). The latter reference also contains data in the critical region.
[101]Smith *et al.* reported (Ref. 80) $\xi = 3.0\epsilon^{-0.57}$ Å for xenon on the critical isochore; however, Smith has found that his data are also consistent with $\xi = 2.0\epsilon^{-0.63}$ Å (private communication). Since the latter value for the correlation length exponent is closer to the value measured in experiments on other fluids we have assumed $\nu = 0.63$ in the present analysis.
[102]A. Michels, A. Botzen, and W. Schuurman, Physica (Utrecht) 20, 1141 (1954).
[103]W. J. Bebach and G. Thodos, Ind. Eng. Chem. 50, 1095 (1958).
[104]J. G. Giddings, Ph.D. thesis (Rice University, 1963) (unpublished).
[105]J. C. McCoubrey and N. M. Singh, Trans. Faraday Soc. 53, 877 (1957); E. S. Wu and W. W. Webb have recently obtained $\eta_s(\rho_c, T_c) = 425 \pm 15$ μP from surface-wave scattering experiments on SF_6 [Phys. Rev. A 8, 2065 (1973)].
[106]P. Calmettes, I. Laguës, and C. Laj, Phys. Rev. Lett. 28, 478 (1972); J. Phys. (Paris) Suppl. 33, C1-121 (1972).
[107]G. Arcovito, C. Faloci, M. Roberti, and L. Mistura, Phys. Rev. Lett. 22, 1040 (1969).
[108]J. C. Allegra, A. Stein, and G. F. Allen, J. Chem. Phys. 55, 1716 (1971).
[109]J. V. Sengers, in *International Centennial Boltzmann Seminar on Transport Phenomena*, American Institute of Physics Conference and Symposium Series, edited by J. Kestin, Vol. 11 (1973).
[110]The system which exhibits the largest difference between theory and experiment is 2,6 lutidine-water, for which the experimental values of Γ^* are approximately 20% smaller than the theoretical values; however, in addition to the large scatter in the linewidth data for this system there are also large uncertainties in the correlation lengths [E. Gulari (private communication)].
[111]See the discussion of the statistical accuracy of digital autocorrelation measurements by E. Jakeman, E. R. Pike, and S. Swain [J. Phys. A 4, 517 (1971)].
[12]L. Mistura, J. Chem. Phys. 55, 2375 (1971).
[113]R. B. Griffiths and J. C. Wheeler, Phys. Rev. A 2, 1047 (1970).
[114]A differential technique was also used by V. G. Puglielli and N. C. Ford, Jr., to determine ξ and κ_T for SF_6 from measurements of the intensity transmitted by the sample [Phys. Rev. Lett. 25, 143 (1970)].
[115]See the discussion by K. Kawasaki between Eqs. (31) and (32) in *Critical Phenomena in Alloys, Magnets, and Superconductors*, edited by R. E. Mills, E. Ascher, and R. I. Jaffe (McGraw-Hill, New York, 1971), p. 489.
[116]See the discussion following Eq. (4) of R. A. Ferrell, Phys. Rev. Lett. 24, 1169 (1970).